



Remote sensing data assimilation

Akhilesh S. Nair, Rohit Mangla, Thiruvengadam P & J. Indu

To cite this article: Akhilesh S. Nair, Rohit Mangla, Thiruvengadam P & J. Indu (2020): Remote sensing data assimilation, Hydrological Sciences Journal, DOI: [10.1080/02626667.2020.1761021](https://doi.org/10.1080/02626667.2020.1761021)

To link to this article: <https://doi.org/10.1080/02626667.2020.1761021>



Accepted author version posted online: 14 May 2020.



Submit your article to this journal



View related articles



View Crossmark data

Publisher: Taylor & Francis & IAHS

Journal: *Hydrological Sciences Journal*

DOI: 10.1080/02626667.2020.1761021

Remote sensing data assimilation

Akhilesh S. Nair^a, Rohit Mangla^a, Thiruvengadam P^a, and J. Indu^{a,b}

^a*Department of Civil Engineering, Indian Institute of Technology Bombay, Mumbai, India*

^b*Interdisciplinary Center for Climate Studies, Indian Institute of Technology Bombay,
Mumbai 400076, India*

Correspondence: J. Indu; indusj@civil.iitb.ac.in; Tel: +91-022-2576-9304

Abstract

Data assimilation (DA) offers immense potential for uncertainty identification, improving the initial estimates for hydrological and atmospheric modelling. This paper reviews the studies in hydrological DA using Kalman filters. Recent applications of Kalman filters in hydrological and atmospheric DA are summarized. Existing challenges for DA studies are briefly described. In addition, three case study examples are presented highlighting the effects of: (a) soil moisture DA in the Noah land surface model; (b) variational assimilation for improving precipitation forecasts in the WRF (Weather Research Forecast) model; and (c) simulating AMSR-2 (Advanced Microwave Scanning Radiometer-2) radiances towards DA. Although there are many unresolved issues in DA that warrant further research, it has immense potential for predicting variables at a better lead time for hydrometeorology.

Keywords

remote sensing; data assimilation; land surface model (LSM); Weather Research Forecast (WRF); radiance

1 Introduction

One of the most challenging practical problems to be addressed by hydrologists and meteorologists is forecasting of key hydrological variables and processes at better lead times. The efficiency of any model to make accurate predictions are largely determined by knowledge of initial conditions (for example, soil moisture in hydrology), our ability to realistically represent the hydrological processes over the forecast period and the quality of forcing data (from climate models or numerical weather prediction models). Information about initial hydrological conditions essentially forms part of the measurement problem

(Lettenmaier, 2017). The challenge in nowcasting and forecasting is how best to combine observations, hydrological models and atmospheric forecasts (Lettenmaier 2017). The solution lies in data assimilation (DA) techniques initially used in numerical weather prediction (NWP) and now in ocean and hydrological sciences too (Reichle et al., 2002a).

Data assimilation was first implemented in the 1950s for numerical weather prediction. Until the 1990s, hydrologists had not paid serious attention to DA (Evensen 1994b, McLaughlin 1995). An efficient use of DA has the potential to handle modelling uncertainties which stem from model inputs, model structures and parameters (Vrugt et al. 2006, Liu and Gupta 2007). The forcing data used, such as multi-satellite precipitation products, may themselves be subject to uncertainties (Indu and Kumar 2014a, 2014b, 2015, 2016; Nair and Indu 2017; Pradhan and Indu, 2019; Ganesh et al., 2019). Some of the most commonly used assimilation techniques are ensemble Kalman filters (EnKF) and three- and four-dimensional variational assimilation systems (3DVAR/4DVAR). In the 1980s and early 1990s, the use of Kalman filter-based DA was examined in meteorology (e.g. Ghil et al. 1989, Cohn and Parrish 1991, Daley 1995).

The current research interest is to improve the efficiency of assimilation in the field of atmospheric sciences and hydrology. In this article, we present three different case studies on the utility of DA to solve different problems in the field of hydrometeorology. A comprehensive literature review of DA studies in hydrology is given in Section 2; a brief glimpse of DA in atmospheric sciences is outlined in Section 3; and Section 4 briefly describes DA methods focused on the EnKF approach. Three different case studies are presented in sections 5, 6 and 7, highlighting the importance of DA in hydrology and meteorology. This is followed by few open-ended questions in Section 8.

2 Data assimilation in hydrology

Within the hydrological community, DA studies focus on assimilation of a single data type (such as soil moisture or streamflow), wherein the spatial resolution of the assimilated observations is the same as that of the model output (Dechant and Moradkhani, 2011; Montzka et al., 2012; Moradkhani et al., 2012; Parrish et al., 2012; Vrugt et al., 2013; Abaza et al., 2014a; Yan et al., 2015; Nair and Indu 2016, 2018, 2019). There are also studies on

assimilated single data type/variables, with a difference in the spatial resolution between the assimilation observation scale and the model output (Reichle and Koster, 2004; Yan et al., 2015). The current trend is to assimilate more than one data type using data from a combination of different satellite sensors and *in situ* data (Lee et al., 2011; Brocca et al., 2012; De Lannoy et al., 2013; Draper et al., 2012; Kumar et al., 2015; Samuel et al., 2014; Wanders et al., 2014).

In hydrology, DA has been carried out using different observations, such as satellite-based soil moisture (e.g. Pauwels et al., 2006; Reichle and Koster, 2005; Brocca et al., 2010, 2012; Liu et al., 2012; Sahoo et al., 2013), land surface temperature (e.g. Caparrini et al., 2004a, 2004b; Sini et al., 2008; Meng et al., 2009; Reichle et al., 2010;), evapotranspiration (e.g. Schuurmans et al., 2003; Pipunic et al., 2008; Irmak and Kamble 2009), streamflow (Seo et al., 2003; Vrugt et al., 2006; Clark et al., 2008; Komma et al., 2008; Seo et al., 2009; Moradkhani et al., 2012; Rakovec et al., 2015; Coustau et al., 2013; McMillan et al., 2013; Abaza et al., 2014b; Noh et al., 2014 ; Rafieeinab et al., 2014 ; Mazzoleni et al., 2015; Li et al., 2015; Rakovec et al., 2015), snow cover (e.g. Clark et al., 2006; Liston and Hiemstra, 2008; De Lannoy et al., 2012b) and vegetation characteristics (e.g. Fang et al., 2011; Ines et al., 2013). Below, some of the key variables used in hydrological DA are summarized.

2.1 Soil moisture

Soil moisture plays a dominant role in the partitioning of incoming radiation into sensible heat and latent heat flux. The prediction skill of coupled land–atmosphere models relies on accurate land surface state initialization, particularly soil moisture (SM). An accurate estimation of antecedent SM conditions plays a critical role in studies involving streamflow simulation (Reichle et al. 2002a, Chen et al. 2013, Wanders et al. 2014) and weather forecasting (Koster et al, 2006). Remote sensing imagery in different regions of the electromagnetic spectrum has resulted in the availability of SM data at unprecedented spatial and temporal resolutions across different scales (Njoku et al., 2003; Entekhabi et al., 2010; Kerr et al., 2010). As a result, studies involving direct assimilation of remotely sensed SM have been receiving increasing attention (Kumar et al., 2014, 2015; Han et al., 2015; Yan et al., 2015; Nair and Indu, 2019).

In the last decade, studies have efficiently assimilated microwave satellite products to improve SM estimates from land surface models (LSMs). This is owing to the high sensitivity of microwave satellite observations to surface SM and relatively low revisit time.

These observations are classified into two types depending on the technique adopted for retrieval: (a) passive microwave observations, which are available from satellites such as the Advanced Microwave Scanning Radiometer for Earth observation science (AMSR-E) (Njoku et al., 2003), the European Space Agency (ESA) Soil Moisture Ocean Salinity (SMOS) mission (Kerr et al., 2010) and the NASA Soil Moisture Active Passive (SMAP) mission (Entekhabi et al., 2010); and (b) active radar observations, such as the two European Remote-Sensing Satellite scatterometers (ERS-1 and ERS-2) (Lecomte 1998) and the Advanced Scatterometer (ASCAT) (Figa-Saldana et al., 2002) on the Meteorological Operational Platform missions (Metop-A, Metop-B and Metop-C).

Previous studies have assessed the potential of satellite SM retrieval for improving LSM state estimates (Reichle and Koster, 2005, Draper et al. 2012; Pan et al. 2012; Lievens et al. 2015b; Nair and Indu, 2016; 2019) assimilated SM from the Soil Moisture Operational Products System (SMOPS) observations using EnKF over India. Reichle et al. (2002a) assimilated L-band microwave brightness temperatures into an LSM to indirectly estimate SM. Other studies have assimilated surface soil moisture and soil wetness index from AMSR-E (Alvarez-Garreton et al. 2014), and surface and root zone soil moisture from ASCAT (Brocca et al. 2012). Previous studies have evaluated the ability of DA using synthetic experiments over the Southern Great Plain (SGP), USA, such as the study by Dunne and Entekhabi (2004), who assimilated the soil moisture in Little Washita and del Reno stations; Yang et al. (2015) examined the same over the Tibetan Plateau and the Mongolian Plateau; similarly, Rodell et al. (2004) studied the effect of soil moisture DA on a global scale using four different LSMs of Global Land Data Assimilation System (GLDAS), namely the Noah, VIC, CLM and CATCHMENT models.

The literature review suggests several such studies that evaluate the impact of soil moisture assimilation on hydrological simulations. However, still, the hydrological DA community is striving to efficiently extract the complete information from the remote sensing-based soil moisture estimates. This is mainly due to the loss in observation information during the conventional bias correction technique done before the assimilation process (Kumar et al., 2015). During this process, the climatology of the observation is converted to the model states to eradicate the bias between them. This is a key step in assimilation as it underpins the critical assumption of unbiased observation and model state. Conventional bias correction techniques, such as the cumulative distribution function (cdf) matching approach, miss out important information in the soil moisture observations (Kumar et al., 2014, Nair and Indu, 2019). Such information is mostly the signals from un-modelled processes such as irrigation

and uncertainty in model forcing (Nair and Indu, 2019; Blankenship et al., 2018). In spite of the limitation in the conventional bias correction approach, studies have successfully retained the irrigation information and used it in the assimilation process (Kumar et al., 2014, Nair and Indu, 2019). The loss in information is also predominant in the processing steps of the blended soil moisture products. One such example is the relatively low irrigation information in the ESA Agency Climate Change Initiative (ESA CCI) blended soil moisture product, as reported in previous studies (Kumar et al., 2014, Nair and Indu, 2019). This loss in the information mainly occurs during the cdf matching technique used to convert satellite SM data to GLDAS climatology (Liu et al., 2012). Therefore, such products have limitations in applications-oriented studies in improving un-modelled processes such as irrigation through data assimilation (Nair and Indu, 2019). With the availability of efficient and advanced techniques, new methods are to be implemented for blending multi-satellite SM products without losing the information in satellite observations. With the availability of low-frequency observations from various satellites, different studies have evaluated the direct assimilation of brightness temperature (Tb) measurements as a proxy for soil moisture. Such studies have indicated considerable improvement in LSM simulation skills using direct assimilation of microwave Tb instead of SM (Tian et al. 2010, De Lannoy et al 2013a; Lievens et al., 2015a).

To facilitate direct Tb assimilation, an LSM is coupled to a radiative transfer model (RTM). Which serves as a forward operator for simulating satellite Tb using the LSM predicted states, such as SM and temperature. The crucial advantage of this method is that it bypasses the need to process data to obtain SM using auxiliary parameters and, hence, avoids the cross-correlated error. However, Tb simulations are highly sensitive to RTM model parameters wherein uncertainty in these lead to degrading the efficiency of DA (De Lannoy et al. 2013a, Lievens et al. 2015a; Nair and Indu, 2016). Therefore, a bias in RTM can lead to an erroneous update in SM during the analysis stage of data assimilation. The RTM simulations are particularly sensitive to topographic effects over hilly terrains. However, in the conventional RTMs used as a forward operator for assimilation, the topographic effect is neglected, which results in bias over hilly terrains. This problem has been recently addressed in a study by Nair and Indu (2018), in which the topographic effect is incorporated into the forward RTM. This RTM reduces the bias imparted from the topographic effect, which helps to improve the efficiency of assimilation. In spite of various studies on RTM parameterization, there is a lack of parameterization schemes that can work efficiently on a

regional scale. This is crucial as the efficiency of assimilation on a regional scale will completely depend on an unbiased RTM.

One of the major concerns in the satellite remote sensing-based measurements is the availability of just surface or near-surface soil moisture (Moradkhani 2008, Han et al. 2012). Chen et al. (2011) argued that DA using surface SM will have a negligible effect on the simulation of SM in the deeper layers. Houser et al. (1998) state that existing SM data from remote sensing need to be complemented with *in situ* surface and root zone observations for proper calibration of model parameters. Draper et al. (2011) show that addressing the reasons for model bias can prove more beneficial than relying on DA. The concept of assimilating remotely sensed soil moisture data remains an active area of research to tackle open-ended questions, such as rescaling issues (Kaheil et al. 2008, Sahoo et al. 2013), uncertainty (Alvarez-Garreton et al. 2014), radiative transfer modelling (Verhoef and Bach 2003, Reichle 2008). A comprehensive explanation of the limitations of soil moisture DA can be found in Vereecken et al. (2015). To date, research is still ongoing to understand certain key areas of the assimilation framework (Brocca et al., 2010; Massari et al., 2015, Alvarez-Garreton et al., 2014).

2.2 Snow

Snow water equivalent (SWE) obtained using satellite remote sensing offers indispensable information to improve the accuracy of streamflow predictions during melting in data-sparse regions. This is especially critical in the north-central USA, which is subject to flooding during periods of snowmelt (Perry 2000). Passive sensors provide Tb which is used to derive SWE and these have been used in snowpack analysis, assimilation into snow models (Andreadis and Lettenmaier, 2006; Pulliainen, 2006, Dong et al., 2007; Durand and Margulis, 2007, 2008; De Lannoy et al., 2012; Kuchment et al., 2010; Dechant and Moradkhani, 2011). Andreadis and Lettenmaier (2006) assimilated AMSR-E data in the VIC model over the Snake River basin in Idaho, USA, and found very little improvement in modelling SWE magnitude. De Lannoy et al. (2012) assimilated AMSR-E SWE into the Noah LSM and showed that, for shallow snowpacks, an improved SWE simulation can be observed. The literature presents studies focusing on direct assimilation of microwave Tb in order to bypass the need to invert Tb into SWE measurements (e.g. Durand and Margulis, 2007; Dechant and Moradkhani, 2011,).

One of the most straightforward means of data assimilation is known as direct insertion. Here, the SWE is replaced by observations at the same location (Liston, 1999, Fletcher et al.,

2012). The direct insertion method avoids the uncertainty of the model and observations. DA approaches using evolving error statistics have been used for snow simulations (Andreadis and Lettenmaier, 2006; Slater and Clark, 2006; Leisenring and Moradkhani, 2011, De Lannoy et al., 2012). Liu et al. (2012) stated that updating of snow accumulation and snowmelt in the snow states has the possibility of improving snow data assimilation methods. Assimilation of SWE has the potential to improve hydrological prediction (Walker et al., 2003). Andreadis and Lettenmaier (2006) assimilated snow observations from MODIS to update the SWE using a VIC model. Clarke et al. (2006) argued that assimilation of snow-covered area results in only a mild improvement in streamflow simulations during the snowmelt season. An extensive description of the topic can be found in the literature (e.g. Pan et al. 2003, Sheffield et al. 2003, Rodell and Houser 2004, Kumar et al. 2008, Parajka and Blöschl 2008). Crow and Wood (2003) assimilated airborne Tb measurements into a TOPMODEL based land atmosphere transfer scheme (TOPLATS).

2.3 Streamflow

Does the forecasting skill of streamflow improve during assimilation of satellite soil moisture? This is an open ended question in the research community (Scipal et al., 2005; Parajka et al., 2006, Crow and Ryu, 2009, Brocca et al., 2010, Chen et al., 2011; Alvarez-Garreton et al., 2014). The usual approach is to use measurements of *in situ* discharge data for assimilation, as they offer superior quality measurements with a better temporal scale. Streamflow observations have also been used to update the model states (Clark et al., 2008, Komma et al., 2008; Noh et al., 2013, Li et al., 2015). Thirel et al. (2010a, 2011b) presented the streamflow assimilation results in an operational forecasting chain over France. Komma et al. (2008) and Coustau et al. (2013) assimilated streamflow data and used a distributed hydrological model to quantify improved predictions at the basin outlet.

Over the past decades, efforts have focused on improving streamflow forecasting using assimilation (Anctil et al. 2003, Yu and Chen 2005, Broersen 2007). The approach followed was to update the streamflow forecast using errors calculated using an independent model, for example, ANN (Anctil et al. 2003), ARIMA (Wang et al. 2015). In hydrological DA, streamflow is not updated directly (Clark et al. 2008; Coustau et al. 2013) and is considered as a diagnostic variable. Direct assimilation of streamflow involves the issue of routing and as such its assimilation follows a slightly different approach to that of other variables. In distributed hydrological models, assimilation of runoff at the current time step requires the current state of the watershed (at the outlet and at other different locations at multiple

previous time steps) to be updated and propagated forward (Pauwels and De Lannoy 2006). Some authors ignore the intricate details concerning channel network to reduce the complexity of the problem (Weerts and El Serafy 2006, Clark et al. 2008). Streamflow assimilation continues to remain an upcoming research area, as it offers unique challenges and common issues to implement the same in operational forecast studies (Andreadis and Lettenmaier 2006).

Hydrologists are highly interested in the proposed Surface Water and Ocean Topography (SWOT) mission to find solutions to all the above-mentioned problems through the assimilation of water-level observations. The SWOT mission is jointly developed and managed by the US National Aeronautics and Space Administration (NASA) and the French space agency, *Centre nationale d'études spatiales* (CNES), in partnership with the Canadian Space Agency and the UK Space Agency. It will revolutionize hydrological observations from space, as it carries wide swath Ka-band radar. The observations from the SWOT mission will radically improve the simulation skills of hydraulic models by assimilating one of kind information. Studies have reported considerable improvement in the river discharge estimates after the assimilation of synthetic SWOT data measurements (Munier et al., 2014, Hind et al., 2018a; 2018b). Therefore, with the launch of the SWOT mission (proposed in April 2022), it is expected that new measurements will be available to improve hydrological forecasting and water management.

2.4 Evapotranspiration

Evapotranspiration (ET) controls the partitioning of energy among the atmosphere, hydrosphere and biosphere. As such, its accurate estimation remains crucial for various areas of hydrology and climate change study. Even though hydrological models allow continuous simulation of catchment-scale ET, their reliability is constrained by the errors in model structure, parameters and initial conditions (Renard et al., 2010; Zhou et al., 2017). Remote sensing provides ET estimates at catchment level with high spatial and temporal resolutions, but these may also contain discontinuities (Velpuri et al., 2013).

Existing studies on ET data assimilation have been conducted at both regional and global scales (Pipunic et al., 2008; Xu et al., 2014). In brief, Shuurmans et al. (2003) used the Surface Energy Balance Algorithm for Land (SEBAL) model and a Kalman filter-based DA algorithm to obtain improved ET estimates; Pan et al. (2008) used a particle filter ensemble Kalman filter to obtain probabilistically optimal ET estimates; Pipunic et al. (2008) used a DA scheme to estimate latent heat flux and sensible heat flux; Qin et al. (2008) stated that use

of extended Kalman filter-based DA resulted in accurate ET estimates but these were unable to improve the hydrological variables; Xu et al. (2014) used a variational DA scheme to get improved estimates of sensible and latent heat flux estimates; Yin et al. (2016) argued that DA improved ET estimates but resulted in adding model error; and Zhou et al. (2017) performed catchment-scale ET assimilation and showed that the proposed technique provided an accurate time series of ET over the Upper Huai River basin, China. There is a strong need to extend ET data assimilation from the regional or global scale to a catchment scale pertaining to hydrological studies.

An interesting point of discussion is whether the assimilation of a single variable improves the estimation of other related variables. For example, Trudel et al. (2014) argued that assimilation of streamflow at the watershed outlet will affect the soil moisture estimates. Often, a combined assimilation of more than one variable is known to provide reliable results compared to that of a single variable (Xie and Zhang 2010, Trudel et al. 2014). With the development of different global and regional land assimilation systems (Cosgrove et al. 2003, Mitchell et al. 2004, Rodell et al. 2004, Kumar et al. 2008), it is now possible to use multi-assimilation schemes using observations from various sources to create an optimal land surface observation. Even though land data assimilation systems offer standalone operation, a major question revolves around whether they need to be coupled to atmospheric models (Walker et al. 2003) for better performance.

3 Data assimilation in atmospheric sciences

Numerical weather prediction (NWP) models represent the present, past and future of atmospheric systems by solving partial differential equations using numerical techniques with a certain order of accuracy. To accurately forecast the weather, the NWP model requires an accurate initial condition that precisely represents the present status of the atmospheric system. Data assimilation is a powerful mathematical technique to generate the best initial condition (status of the atmosphere) using available observation data. Atmospheric data assimilation started with the work of Richardson (1922) and Charney *et al.* (1950), who calculated the present state of the atmosphere based on manual interpolations. This assimilation process was very tedious and other researchers (Panofsky, 1949, Gilchrist and Cressman, 1954; Cressman, 1959; Barnes, 1964) developed an objective analysis method with the aid of computers. Some of the first-generation objective analyses were functioned fitting (Panofsky, 1949, Gilchrist and Cressman, 1954), successive correction method

(Bergthórsson & Döös, 1955, Cressman, 1959) and optimal interpolation (Gandin, 1966). The observational data used for assimilation were from surface observations and radiosonde at synoptic times.

Since 1965, the meteorological observational network has become very complex, with a lot of asynoptic observations from aircraft reports, drifting buoys, geostationary and polar-orbiting satellites and so on. Assimilation of these observations using the objective analysis method was very challenging. To meet this challenge, Charney and Drazin (1961) and Hoke and Anthes (1976) proposed direct insertion and nudging methods, respectively, to assimilate asynoptic observations. One of the major disadvantages of these methods is that they are both empirical methods and lack a theoretical basis of statistical estimation. In 1980, new data assimilation methods, such as 4D variational systems (4DVAR) and Kalman filter emerged. The area of research in these two techniques has seen tremendous growth and development in data assimilation for NWP models. The 4DVAR technique has been also adapted at major operational centres (the European Centre for Medium Range Weather Forecast, ECMWF, and centres in France, UK, Japan and China) for initializing NWP. However, the computational cost of 4DVAR is very high due to its strong dependence on the highly complex adjoint model of the forecast model. In addition, it is very difficult to develop adjoint models for certain model physics which involves substantial on-off processes (Xu, 1996, Zou, 1997, Steward *et al.*, 2012). These limitations have increased the demand for the development of more efficient methods such as EnKF and some nonsmooth optimization techniques (Emrouznejad, 2016). Even though EnKF has become highly competitive with 4DVAR, its performance is still limited by sampling errors, caused by limited sample sizes. The field of atmospheric data assimilation has been constantly evolving through the efforts of research and operational centres around the world. However, the operational weather models use billions of variables to forecast the weather but typically assimilate only millions of observations. Over the past decades, there has been an increase in diverse atmospheric observations from different remote sensing platforms such as satellites and Doppler Weather Radars (DWR), which provide dense information about the convective-scale phenomena at suitable temporal and spatial resolutions. These observations are not fully exploited in the atmospheric data assimilation systems, with only a very small fraction of satellite observations currently being used operationally. Studies by Xiao *et al.* (2005), Hu *et al.* (2006), Sun *et al.* (2012), Wang *et al.* (2012) and Tong *et al.* (2016) have shown the impact of assimilating DWR observations in improving the quality of initial condition supplied to the

weather models. Some of the operational centres, such as the Korean Meteorological Centre (Xiao *et al.*, 2008), the UK Met Office (Ballard *et al.*, 2005) and the NCEP operational data assimilation system (Alpert and Kumar, 2007), have adapted assimilation systems for Doppler radial wind observations to improve the skill of weather forecasts. Over the Indian region, DWR are most commonly used to improve the tracking forecast of cyclones (Routray *et al.*, 2005, Abhilash *et al.*, 2012, Osuri *et al.*, 2015). There are only a few studies (Routray *et al.*, 2013, Thiruvengadam *et al.*, 2019,2020) that have addressed the problems in convective-scale precipitation forecasting over the Indian region by assimilating DWR observations. Nevertheless, no operational application of DWR data assimilation has been performed over the Indian region. One of the major problems that affects the skill of DWR data assimilation is the quality of covariance matrix used to weight the previous forecasts. Thiruvengadam *et al.*, (2019, 2020) analysed the sensitivity of covariance matrix in a 3DVAR based DWR assimilation system for predicting a heavy rainfall event that occurred over the southeastern part of India. Although all of the studies which used DWR assimilation have demonstrated success, operational implementation of DWR assimilation poses a number of challenges. Studies on designing a robust strategy for operational implementation of Indian DWR data assimilation are essential. In addition to ground-based observations, the huge database of satellite observations has been extensively used in variational data assimilation to infer the initial state of the atmosphere in NWP models and these are capable of producing better forecast skills (Geer *et al.*, 2012, Geer, 2013). In the last three decades, the framework of satellite data assimilation has moved a step ahead from assimilating retrieved variables, e.g. temperature and water vapour profiles from sounders (Eyre *et. al.*, 1993; Tauchi *et al.* 2004) to direct radiances at operational NWP centres (Geer *et al.* 2018). Now, the current status of development is moving towards clear-sky assimilation to an all-sky (clear and cloudy) approach with the aim to use cloud and precipitation information in forecast analysis. With the clear-sky approach, a large percentage of data are screened out in preliminary analysis due to cloud contamination (McNally and Watts 2003). Geer et al. (2011) developed a symmetric error model for all-sky observation errors by taking into account the cloud and precipitation affected radiances. This approach allows us to assimilate all-sky observations if errors are treated correctly. Okamoto et.al (2017) used the same model to evaluate the all-sky Himawari-8/AHI infrared radiances in perspective to assimilate in regional mesoscale NWP models.

In the ECMWF NWP model, microwave radiances from Special Sensor Microwave Imager Sounder (SSMIS) (Kunkee *et al.*, 2008), Tropical Rainfall Measuring Mission (TRMM)

Microwave Imager (TMI) (Kummerow *et al.*, 1998), Advanced Microwave Scanning Radiometer-2 (AMSR-2) (JAXA, 2013) and Advanced Microwave Sounding Unit-A (AMSU-A) (Geer *et al.*, 2012) are assimilated in all-sky conditions (Geer, 2013, Kazumori *et al.*, 2014), whereas the regional Weather Research Forecast (WRF) model still uses clear-sky MW radiances for assimilation (Routray *et al.*, 2016, Singh *et al.*, 2016). The all-sky assimilation uses a fast and accurate radiative transfer (RT) model (for e.g. RTTOV) that is capable of simulating the scattering and absorption effect of convective hydrometeors. Previous works found the several complicated issues that affected the assimilation, such as complicated non-linear cloud processes, non-Gaussian characteristics of observed-minus-background (O-B) and inaccurate modelling of clouds in RT models (Geer *et al.*, 2018, Okamoto, 2017). Among all issues, poor modelling of cloud and precipitation scattering effects in RT models produces large errors which can degrade the quality of assimilation (Geer *et al.*, 2012).

In traditional data assimilation, observations and background (i.e. model forecast in radiance space) are combined with their respected errors to produce the best analysis (Waller *et al.*, 2016). Therefore, the accuracy of analysis relies on observation, background and the RT model. The errors in model simulations in cloudy regions largely depend upon the shape of frozen hydrometeors, assuming the density and particle size distributions are fixed (Geer and Baordo, 2014). In this context, the third case study investigates the impact of spherical as well as non-spherical shapes of frozen hydrometeor on radiance simulation towards all-sky assimilation.

4 DA methods

Data assimilation (DA) algorithms aim at synergistically combining imperfect model predictions and observations to obtain an optimal solution. The approaches to solve this problem are classified as direct observer technique, dynamic observer technique and hybrid technique.

4.1 Direct observer technique

In this assimilation technique the model forecasts are updated sequentially whenever observations are available. This is achieved by calculating the difference between observations (Z) and model predicted observations (z), known as innovation, where the predicted observations are estimated from the model forecast. During the assimilation stage, the model forecast (X^b) is updated closer to the observation based on innovation multiplied by

a weighting factor K known as Kalman gain. The Kalman gain depends on the relative uncertainty in the observation and model variances, which is a number between 0 and 1. The updated state is known as the analysis state (X^a):

$$X^a = X^b + K(Z - z) \quad (1)$$

The different approaches for direct observer assimilation techniques are summarized below.

4.1.1 Direct insertion

This is one of the oldest data assimilation methods. In this method the most crucial assumption is that the model predictions are incorrect and the observations are perfect, hence the forecast model states are directly replaced with the observation. The disadvantage of this method is that it disregards the crucial information provided by the model forecast and preserves the observation errors (Houser et al. 1998).

4.1.2 Statistical correction

This is a modified version of the direct insertion approach, in which it is assumed that the model predictions are true with uncertainties. These uncertainties are reduced by adjusting the mean and variance of the model states to match the observations (Houser et al., 1998).

4.1.3 Successive correction method

In this method, the model forecast states are modified by the observations in an iterative manner. In the first step of the successive correction method, the model forecast at every grid point is updated based on the model first guess and the observations surrounding that grid point with a certain weightage. After a first pass of model state correction, another pass is made, again modifying the field at each grid point based on the observations surrounding the grid point. The two commonly used successive correction methods are the Cressman scheme and the Barnes scheme (Bratseth, 1986).

4.1.4 Nudging

The nudging data assimilation method adopts dynamical relaxation by adding a term to the prognostic model equation that causes the solution to be gradually relaxed towards the observation state (Stauffer and Seaman, 1990).

4.1.5 Optimal interpolation

This is one of the most widely used least squares methods of data assimilation. The least squares method differs from successive correction and nudging methods in that the observations are weighted according to some known or estimated statistic regarding their errors, rather than by using empirical values. Thus, observations from different sources can be weighted differently based on known instrumental and other errors. The optimal

interpolation method attempts to minimize the total error of all the observations to come up with an optimal weighting for the observations. This method allows a more scientific and flexible way of including observations from different sources (Lorenc, 1981).

4.1.6 Kalman filter

The Kalman filter approach of data assimilation utilizes the dynamic updating of the forecast error covariance through time. In the traditional Kalman filter (KF, Kalman 1960) approach the error covariances are computed from standard error propagation theory using a linear model. Two frequently used adaptations to the KF approach are the Extended KF (EKF, Puente and Bras 1987) and the Ensemble KF (EnKF, Evensen 1994). In EnKF, the covariances are calculated from an ensemble of state forecasts. The EnKF algorithm has been widely used in different land surface data assimilation studies.

The EnKF approach of DA is a Bayesian filtering process, which alternates between an ensemble forecast stage and a state variable update stage (Fig. 1). During the ensemble forecast stage, the model propagates forward in time with a predefined ensemble size, while, in the variable update stage, the simulated states are updated closer to observations. The model states are updated closer to observations as follows:

$$\mathbf{U}_{i,j}^t = F_{i,j}^t + \mathbf{K}(\mathbf{Z}_{i,j}^t - H\mathbf{z}_{i,j}^t) \quad (2)$$

where i is the grid number; j is the ensemble number; $\mathbf{U}_{i,j}^t$ is the updated model states vector; $\mathbf{z}_{i,j}^t$ is the forecast states; $\mathbf{Z}_{i,j}^t$ is the observation state vector; and \mathbf{K} is the Kalman gain matrix, which depends on forecast error variances ($C_{\psi\psi i}^t$) and measurement error variance ($C_{\omega\omega i}^t$):

$$\mathbf{K} = \frac{C_{\psi\psi i}^t H_i^{tT}}{H_i^t C_{\psi\psi i}^t H_i^{tT} + C_{\omega\omega i}^t} \quad (3)$$

which are computed in EnKF algorithm from perturbed observed and land surface states. This is achieved by applying additive and multiplicative uncertainty on meteorological forcing inputs, model estimated state variables and observations.

4.1.7 Three-dimensional variational method (3DVAR)

This scheme applies an iterative minimization problem to obtain an optimal solution. It uses statistic background error covariance matrix approximation, the same as in the optimal interpolation scheme. Implementation of the 3DVAR technique in the WRF model (WRF-3DVAR) is a variational data assimilation system developed for the WRF model. The system originated and evolved from the work of Barker et al. (2004) on the fifth-generation Pennsylvania State University – National Centre for Atmospheric Research Mesoscale Model (MM5) 3DVAR system. The main goal of the WRF-3DVAR system is to produce a better

initial condition to the WRF model through an iterative solution of a prescribed cost function (Ide et al. 1997). The cost function produces an optimum comparison between the prior estimation of analysis field and observations, weighted by their respective errors. The iterative minimization process in 3DVAR is performed in a preconditioned control-variable space. The major advantage of reducing the cost function in this space is that when the background fields are represented in the control-variable space; its errors are uncorrelated and the variances are of a unit size, which in turn reduces the computation time to a greater extent. The preconditioned control variables include stream function, unbalanced potential velocity, unbalanced temperature, unbalanced surface pressure and pseudo-relative humidity. The cost function of 3DVAR is:

$$J(x) = \frac{1}{2} (X - X^b)^T \mathbf{B}^{-1} (X - X^b) + \frac{1}{2} (Z - z^0)^T \mathbf{R}^{-1} (Z - z^0) \quad (4)$$

where x is the analysis to be found to minimize the cost function $J(x)$; x^b is the first guess of the WRF model; \mathbf{B} is the background error covariance matrix; and \mathbf{R} is the observation error covariance matrix.

4.2 Dynamic observer technique

This technique finds the optimal fit between the forecast model and observation state by minimizing an objective function J over a space and time window:

$$J = \frac{1}{2} (X_0 - X_0^b)^T \Sigma_0^{b^{-1}} (X_0 - X_0^b) + \frac{1}{2} \sum_{k=1}^{N-1} (Z_k - z_k)^T R_k^{-1} (Z_k - z_k) \quad (5)$$

where b is the background estimate of the state vector; N is the number of time steps; and K is the time of update. In order to minimize J over time, the derivatives of the objective function with respect to the initial model state X_0 is obtained using an ‘adjoint’ model over a time window. The classical 4D variation assimilation system is a perfect example of dynamic observation technique. The acronym 4D comes from the model set-up and assimilation in three dimensions in space and one dimension in time. This variational assimilation technique uses an adjoint model to trace the trajectories of the objective function with respect to each of the initial state values. It attains the minimization of objective function in multiple iterations. When the 4DVAR method is applied to a perfect model with finite time interval, it yields results similar to the Kalman filter at the end of the assimilation time interval. But, during the course of assimilation 4DVAR performs better as it has all observations at once (pre- and post-time step of analysis) (Houser et al., 2005).

4.3 Hybrid data assimilation

In recent decades, atmospheric DA has garnered significant interest in calculation of an accurate and flow-dependent estimate of background error covariance. To achieve this,

studies have proposed a hybrid assimilation technique. In this technique, the background error covariance matrix is computed from an ensemble-based model in a conventional variational assimilation method. Hence, the hybrid assimilation technique combines the standard variational data assimilation with a localized ensemble-based technique (Hamill and Snyder, 2000, Buehner 2005). A study by Liu et al. (2008, 2009) implemented this technique to compute background error covariance within a time window; this was named 4D-En-Var.

Recent studies on atmospheric data assimilation (Amezcu *et al.*, 2017; Bannister, 2017, Bowler *et al.*, 2017, Gustafsson, 2007, Kalnay *et al.*, 2003; 2007; Lorenc, 2017) have avoided the deficiencies in both 4DVAR and EnKF methods by developing a hybrid method which ideally inherits the advantage of both the methods. Some of the most commonly used hybrid methods are 4DEnKF, EN4DVAR (Zhang *et al.*, 2009) and 4DENVAR (Yang *et al.*, 2006, Liu *et al.*, 2008, Tian *et al.*, 2008, Wang *et al.*, 2010, Tian and Xie, 2012, Tian and Feng, 2015). In the 4DENKF method, the EnKF system is extended to four dimensions as a smoother to assimilate observations at a preferred time step without iterations. The EN4DVAR system utilizes the combination of the ensemble background error covariance from EnKF along with climatological covariance to represent the error in prior data in a 4DVAR assimilation system. However, EN4DVAR still uses an adjoint model for solving the minimization problem which 4DENVAR has avoided by utilizing simulated observation perturbations as an approximate to tangent linear model. One of the open questions in hybrid data assimilation is whether we can achieve a balance between 4DVAR and EnKF in terms of accuracy, computational cost and performance.

5 Case study on soil moisture data assimilation

This case study evaluates the performance of SM assimilation to improve offline LSM spin-up. This is investigated by assimilating the multi-satellite SMOPS product into LSM during spin-up. The EnKF (Reichle et al. 2002a, 2002b) within NASA's Land Information System (LIS; Kumar et al. 2008) is used to assimilate SMOPS observations into the Noah LSM version 3.6 (Ek et al. 2003). The study is conducted over the Indian subcontinent (Fig. 2) on the area between 8.125°N - 37.375°N and 68.125°E - 97.375°E . The LSM is initialized at a spatial resolution of $0.25^{\circ} \times 0.25^{\circ}$ and the study is conducted for a period of two years from 2009 to 2010.

The forcing data for this study stems from National Centers for Environment Prediction (NCEP) operational atmospheric assimilation system known as Global Data

Assimilation System (GDAS; Derber et al., 1991). This product is generated by assimilating surface observations from balloon data, wind profiler data, aircraft reports, buoy observations, radar observations and satellite observations by 4D multivariate approach (Rodell et al. 2004). The study uses a multi-year spin-up loop to initialize the Noah LSM using GDAS forcing. The Noah LSM is based on the Oregon State University (OSU) LSM. This LSM is configured with four layers for soil moisture and temperature and two snow layers. The soil is configured with increasing thicknesses of 10, 30, 60 and 100 cm. Further, it consists of diurnally dependent Penman potential evaporation approach (Mahrt and Ek, 1984) to calculate evaporation and a primitive canopy model based on Pan and Mahrt (1987).

Initialization is a critical component of offline LSM simulation and this is achieved by simulating model for particular time period before actual simulation of model. The model initial states consist of spatially varying land surface water and energy states. The LSM initial states are sensitive to model type, resolution, forcing data, auxiliary parameters and domain. Hence, inappropriate LSM initialization leads to erroneous model state simulations. This study evaluates a multi-year model spin-up method to initialize the Noah LSM as proposed by Rodell et al. (2005). Along with this conventional approach, this study assimilated soil moisture during spin-up.

For this study, SMOPS soil moisture products are assimilated into Noah LSM using the 1D approach of EnKF (Reichle et al., 2003). The efficiency of the EnKF algorithm in improving LSM states though soil moisture assimilation is evident from previous studies (Margulis et al. 2002; Reichle et al. 2002a; Kumar et al. 2015). However, all these studies assimilated soil moisture in LSM after offline spin-up. This approach requires a large computation time for model initialization using spin-up. Hence, to overcome this issue, this study assimilates soil moisture during the spin-up run. Santanello et al. (2016), conducted a similar study on the impact of soil moisture assimilation during LSM spin-up for a coupled land–atmosphere prediction models over the USA. Through this study it is expected that assimilating soil moisture will reduce the spin-up time and result in a realistic surface initialization. The perturbation set-up is followed as in Nair and Indu (2016).

5.1 Experimental set-up

Investigation of the performance of soil moisture assimilation during LSM spin-up is achieved by assimilating soil moisture in Noah LSM version 3.6 using EnKF (Reichle et al. 2002a, 2002b) in the Land Information System (LIS) framework (Kumar et al. 2006).

The soil moisture observations for this study stem from blended SMOPS products (Zhan et al. 2011), which comprise of soil moisture estimates from AMSR-E and Windsat

observations derived using the single channel retrieval (SCR) algorithm. Further, it includes observations from the ASCAT and SMOS missions. This study assimilates SMOPS blended surface soil moisture into Noah LSM during four cyclic spin-up loops from 2009 to 2010. Before assimilation the biases between the model and observations are removed using a lumped cdf matching approach (Reichle and Koster 2003). The cdfs are computed from soil moisture observations and model simulations for each grid point over the 2-year period (2009–2010). The forcing variables (incident shortwave radiation level, incident longwave radiation, rainfall rate) and model states (soil moisture for all four layers) are perturbed with additive and multiplicative Gaussian errors to create 30 model ensembles. The SMOPS observation is used to directly update the model prognostic variables (surface soil moisture). This experimental set-up is adopted from Nair and Indu (2016)

The efficiency of assimilation during spin-up is evaluated using two separate offline simulations. During the first run, hereafter referred as open loop (OL), the model spin-up was performed without assimilation for a period of 8 years by four loops of simulation using GDAS forcing from 2009–2010. The second run, data assimilation (DA), has a similar configuration, but along with SMOPS assimilation. The evaluation results are presented for each spin-up loop for each run. The results are further validated with *in situ* soil moisture observations from the International Soil Moisture Network (ISMN) over the Central Tibetan Plateau (CTP) (Fig. 2, inset).

5.2 Results

The variation of innovation during the spin-up runs depicts the closeness of the simulated mean with observation. Figure 3(a) and (c) presents the monthly mean of innovation for all four spin-up loops over 2009 and 2010, respectively. The difference between loop 1 and subsequent loops is evident, particularly for the starting year 2009. This is owing to the cold-start initialization of LSM with uniform soil moisture of $0.2 \text{ m}^3/\text{m}^3$. As the model runs forward in time, the difference in innovation reduces between consecutive loops. Figure 3(b) and (d) presents the mean innovation for the four loops over 2009 and 2010, respectively. This shows that as the spin-up loops increase the difference in innovation converges.

Figure 4 shows the impact of land data assimilation during spin-up over four layers for the fourth spin-up loop. It is evident that SM assimilation has considerable impact on the first three layers of soil moisture; however, it has the least impact on the last SM layer. This can be attributed to the low correlation between surface and deep layer soil moisture.

Figure 5 depicts the annual mean spatial plots of SM for all four layers. Here, Figure 5(a)–(d) shows mean soil moisture for 2009 from OL simulation, Figure 4(e)–(h) shows mean soil

moisture for 2009 from DA simulation. Similarly, Figure 4(i)–(l) shows simulations from OL for 2010 and Figure 5(m)–(p) shows simulations from DA for 2010. The impact of DA is clearly evident in these plots with variation in SM intensities in DA runs as compared to OL runs. The major difference can be observed in the states of Madhya Pradesh, Maharashtra, Rajasthan, southern Indian peninsula and northeastern states of India. The low impact on the fourth SM layer over the majority of the domain is notable, except for regions with grassland particularly over the northeastern tip of the country.

Furthermore, the results are validated with *in situ* SM over the CTP. Figure 6 (a) and (b) shows daily SM for layer1 for the first and fourth spin-up loops. It should be noted that the Noah LSM performs well over the CTP due to uniform land cover by land class. The DA simulation has values closer to *in situ* observations as compared to the OL run. This is evident particularly between 10 and 15 August 2009, where soil moisture in the DA simulation in loop 4 (Fig. 6(b)) is closer to ISMN observations as compared to loop 1 (Fig. 6(a)). Similar results are obtained for September, as shown in Figure 7.

The results from the offline simulations indicate that there is large increment in SM values throughout the domain. The evaluation results from innovation indicate that as the number of loops increases the innovation values converge. This indicates that the model tends to attain equilibrium in a shorter spin-up time. This is evident from the fact that the innovation attains equilibrium in four loops, while for conventional spin-up (without DA) it takes longer. The results from *in situ* observations over the CTP show that soil moisture assimilation during spin-up brings LSM simulated SM close to observation.

5.3 Conclusion

This case study evaluates the feasibility of assimilation for improving the initialization of standalone LSMs. The results from our analysis indicate that assimilation of soil moisture during the spin-up run reduces the spin-up time. The assimilation characteristics are sensitive to the spin-up runs: the innovation vector converges as the loop increases. These characteristics can be used as criteria for evaluating the stability of the model initialization. This approach will be more reliable to the conventional approach of spin-up as the model states will be constrained to the true observations.

6 Case study on atmospheric data assimilation

Tropical cyclones are one of the most common hazards in the Indian region and cause intense flooding and devastating damage, mainly to coastal areas. For cyclone mitigation and flood forecasting (Ghosh *et al.*, 2019), accurate forecasting of the intensity and track of cyclones is

essential. The major difficulties in the numerical prediction of tropical cyclone tracks and intensity are mainly due to limited physical parameterization, uncertainty in initial and boundary conditions from the global model and error in topographic data (Jianfeng et al., 2005, Subramani et al., 2014). Since the weather models represent the atmospheric dynamics process by solving non-linear equations through various approximations, controlling the error in the model physics can be achieved only to a certain extent. Also, the location of precipitation forecasting mainly depends on the model forcings and only indirectly on the physical parameterizations. Hence, the skill of precipitation forecasts mainly depends on the quality of initial conditions supplied to the NWP model, which can be improved by data assimilation (Arpe et al., 1985; Sun et al., 2012; Zhang et al., 2013). As 4DVAR and hybrid assimilation systems are computationally costly, in this study we tested the effect of a 3DVAR assimilation system (approximation of 4DVAR) in improving the precipitation forecasts. The main aim of this study is to demonstrate the ability of the 3DVAR assimilation technique in improving the precipitation forecasts regardless of the physical parameterizations used in the model.

Past studies, principally over the Bay of Bengal and Indian Ocean regions (eg. Bhowmik and Prasad, 2001; Rajan et al., 2001; Das et al., 2003; Mukhopadhyay et al., 2005; Vaidya et al., 2004; Routray et al., 2005, 2010; Mandal et al., 2006; Sandeep et al., 2006; Vinodkumar et al., 2007, 2008, 2009a, 2009b; Govindankutty et al., 2008; Xavier et al., 2008; Singh et al., 2016) have shown that assimilation of surface and upper air observations using 3DVAR have an overall positive impact on analysis and prediction of tropical cyclones. However there is a gap in analysis of the role of assimilation systems in reducing the uncertainty by model physics options (Thiruvengadam *et al.*, 2019). In this study, we conducted 12 sets of experiments containing non-assimilation (six) and assimilation (six) experiments to analyse the effect of assimilation on reducing the precipitation forecast error due to model physics. The precipitation forecasts from all the experiments are verified against Global Precipitation Measurement (GPM) precipitation observations using forecast skill scores.

The case used in this study is a cyclonic storm named Ockhi that occurred between 29 November and 4 December 2017. According to Indian Meteorological Department, it was a Category 3 very severe cyclonic storm, which intensified from a deep depression to a cyclonic storm in less than 6 h. It was one of the worst cyclones to have struck India in 50 years. A low pressure developed near the southeastern coast of Sri Lanka, in the southwest Bay of Bengal on 28 November 2017. On 29 November 2017, the low pressure concentrated into a depression and began moving northwestward, with a maximum wind speed of 180

kmph (IMD) causing massive destruction over the South Indian region. The uniqueness of this storm is that it intensified from a deep depression to a cyclonic storm within 6 h as this normally takes two days to happen. Accurate NWP forecasting of such rapidly accelerating storms is very challenging. In this study, we analysed how assimilation of conventional observations has a major impact in improving the accuracy of prediction.

6.1 Model characteristics and experimental design

The Weather Research and Forecasting (WRF) model version 3.9 along with an assimilation system is used in this study. A single domain with a spatial resolution of 27 km and a vertical profile with 50 eta levels from the land surface to 10 hPa is used in this study, as shown in Figure 8. The initial and boundary conditions are generated from global forecast data available at $0.25^\circ \times 0.25^\circ$ horizontal resolution and 6-h intervals. To study the sensitivity of cloud physics and convection in forecasting the cyclone, six simulations were performed with a combination of two microphysics options and three cumulus physics options. To analyse the effect of assimilation, six further assimilations were conducted through assimilation of quality controlled surface and upper air observations¹. These observations include radiosonde, land surface, pibal and aircraft reports from the Global Telecommunications System, oceanic winds and total cloud water from the Special Sensor Microwave Imager (SSM/I) and satellite wind data from the National Environmental Satellite Data and Information Service. Thus a total of 12 experiments containing six sets of non-assimilation runs (control) and six sets of assimilation runs (3DVAR) were conducted. The microphysics options used are the Kessler scheme and Lin *et al.* scheme; the cumulus physics options are the Betts-Miller-Janjic scheme (BMJ), Grell 3D (G3) and modified Kain-Fritsch (KFm). The fixed parameterization scheme used is the Yonsei University (YSU) Planetary Boundary Layer, Noah LSM, Rapid Radiative Transfer Model (RRTM) (Mlawer *et al.* 1997) for longwave and Dudhia (Dudhia 1989) shortwave radiation schemes. Table 1 presents a summary of the 12 experiments. In the control experiments, the model is integrated without any data assimilation for 48 h using the initial condition valid at 00:00 UTC on 29 November 2017. The assimilation experiments were based on the assimilation of quality controlled conventional observations at 6-h intervals from 06:00 UTC on 29 November 2017 to 00:00 UTC on 30 November 2017. A 6-h forecast (spin-up) from the initial condition valid at 00:00 UTC on 29 November 2017 is used as a first guess for starting the assimilation cycle. Hence, a total of four assimilation cycles were performed to improve the initial condition, then the

¹ <http://rda.ucar.edu/datasets/ds337.0/>

model was integrated to provide a 24-h forecast valid at 00:00 UTC on 1 December 2017. Figure 9 shows the time bar of WRF cycle runs. The precipitation forecasts are verified using the fractional skill score (FSS) neighbourhood technique developed by Roberts (2005). Global Precipitation Measurement (GPM) rainfall observations were used as truth for verification. The GPM-IMERG, ‘Final’ product, precipitation was interpolated onto a 20-km resolution grid to compute verification statistics; IMERG is one of the GPM products, which provides a multi-satellite rainfall product (Huffman *et al.*, 2017).

Following Robert and Lean (2008), FSS is defined as:

$$FSS = 1 - \frac{FBS}{FBS_{worst}} \quad (6)$$

where FBS is the fractional brier score and FBS_{worst} corresponds to the case where there is no overlap between observed and model fractions. In this study, fractions of model and observations are generated for every grid point by computing the fraction of surrounding points that exceeds 1 mm of rainfall within a 5×5 kernel. A rainfall threshold above 1 mm is chosen to verify the skill of atmospheric data assimilation for all ranges of precipitation. The two parameters are given by:

$$FBS = \frac{1}{N} \sum_{i=1}^N (P_{O(i)} - P_{F(i)})^2 \quad (7)$$

$$FBS_{worst} = \frac{1}{N} [\sum_{i=1}^N P_{O(i)}^2 + \sum_{i=1}^N P_{F(i)}^2] \quad (8)$$

where $P_{O(i)}$ and $P_{F(i)}$ are the fractional values at the i th grid point in the observations and model forecasts, respectively; and N is the total number of grid boxes. The range of FSS varies from 0 to 1, where 1 signifies a perfect forecast and 0 signifies no skill.

6.2 Results

To analyse the impact of conventional DA on precipitation forecasts, the 6-h accumulated rainfall from the control and assimilation experiments is spatially compared with 6-h accumulated GPM observations. For this, GPM rainfall observations with $0.1^\circ \times 0.1^\circ$ spatial resolution are downscaled to model resolution (27 km) using a linear interpolation technique. Figure 10 shows the 6-h accumulated precipitation from the control and the assimilated experiments for the first experiment (Kessler-BMJ). The remaining assimilated experiments are shown in the Appendix (Figs A1–A5). A larger spatial spread of rainfall can be observed in the control experiments with BMJ and G3 as cumulus physics (Fig. 10(a)–(d), Fig. A1(a)–(d), Fig. A3(a)–(d), Fig. A4(a)–(d)). When Global Telecommunication System (GTS) observations² are assimilated for the same experiments (Fig. 10(e)–(h), Fig. A1(e)–(h), Fig.

² <https://rda.ucar.edu/datasets/ds337.0/>

A3(e)–(h), Fig. A4(e)–(h)), a converged spatial pattern of precipitation matching the GPM precipitation can be observed. It is clearly noticeable that each control experiment provides a different spatial pattern of precipitation, whereas an overall similar structure in the spread of precipitation is present in all the assimilation experiments. From these experiments, it can be inferred that assimilation of conventional observations improves the spatial spread of precipitation regardless of the physical parameterization. The statement is further supported using the average FSS boxplots of both control and assimilation experiments. Figure 12 shows the FSS boxplots of control and assimilation experiments for the forecast hours. The values of FSS for all the experiments are shown in Table 2. It can be clearly observed from the FSS boxplots that the spread of forecast skill in assimilation experiments is very low for all the forecast hours when compared to that in the control experiments. Also, in the control experiments, a larger distribution of forecasting skill is found for the 00–06 forecast and then it gradually decreases. It can be also noted that for all the forecasts the average forecast skill of the assimilation experiments is 10–20 % greater than that of the control experiments. These results offer powerful evidence for the positive impact of assimilation on precipitation forecasts. The results further show that the assimilation of conventional observations has improved the quantitative precipitation forecast regardless of the microphysics and cumulus scheme chosen.

6.3 Conclusion

In this case study, the WRF-3DVAR system along with GTS data was used to improve the forecasting skill of precipitation with different parameterized schemes in the WRF model. The precipitation forecasts from the experiments were spatially compared with GPM precipitation datasets. Statistical verification was also performed to quantitatively evaluate the forecast skill of each experiment. It was observed that assimilation of conventional observations improved the spatial spread and structure of the precipitation forecasts. In addition, a significant positive improvement in forecast skill score was observed after assimilation of GTS observations. Overall, it was observed that data assimilated initial conditions show more effective results when compared to the non-assimilated ones.

7 Case study on simulations of all-sky AMSR-2 radiances in RTTOV framework towards DA

The existing literature states that assuming the spherical shapes of snow/ice hydrometeors produces excessive scattering in 30–90 GHz and inadequate scattering at higher frequencies (Hong *et al.*, 2005). Efficient modelling of scattering properties directly influences the radiative properties of temperature and moisture sounding channels (Geer *et al.*, 2012). The 3D discrete dipole approximation (DDA) shapes, such as long column, short column, block-column, thick-plate, thin-plate, 3,4,5 and 6 bullet rosette, sector and dendrite snowflake (Liu, 2008), are added into RTM models and the results are significantly improved in cloud and precipitation regions (Guerbette *et al.*, 2016, Rysman *et al.*, 2016). The availability of AMSR-2 microwave polarimetric measurements at 89V-GHz is strongly affected by scattering from frozen hydrometeors. Yang et al., (2016) performed all-sky AMSR-2 radiance assimilation in the WRF model at frequencies from 10 to 37 GHz. Limited studies have been done over a higher frequency (89 GHz). Investigation of hydrometeor shapes for accurate simulation of clouds at higher frequencies is important as they may produce uncertain scattering and make it complex in NWP models.

There is a lack of such studies focused over India. Routray et al., (2016) implemented MW radiance assimilation to evaluate tropical cyclone forecasts over the Bay of Bengal. They observed the positive impact of assimilation, which improved the track, intensity and structure of storms. Keeping this in mind, the present case study examined the DDA shapes for reproducing all-sky AMSR-2 brightness temperature (BT) at 89 GHz-V over the Indian region.

The data used were AMSR-2 channel 13 (89 GHz-V) radiance, which is sensitive to sea-ice concentration and convective precipitation (Mangla et al., 2020). The WRF (v3.8) model (Skamarock *et al.*, 2008) was run in single domain from 3°–26°N and 73°–103°E, with 213×165 horizontal grids at 15 km grid resolution. The initial and boundary conditions were taken from ERA-5 reanalysis datasets of 31 km spatial resolution at 3-h intervals. Geographical information including land use and land cover (LULC), soil type, topography, lake and vegetation parameters, were used at 30 s resolution from the US Geological Survey (USGS) global datasets. This study used the physical parameterization schemes suggested by Routray et al., (2016) for the Indian region (Table 3).

The all-sky AMSR-2 radiances were simulated from RTTOV-SCATT version 12.1 of the Radiative Transfer model for Television Infrared Observation Satellite Operational Vertical Sounder package (RTTOV) (Hocking *et al.*, 2017, Saunders *et al.*, 2017). The model input required the hydrometeor profiles (cloud water, ice, snow, rain and cloud fraction), humidity

and surface fluxes. The surface emissivity over ocean is provided by the FASTEM version 6 model (Kazumori and English, 2015). For this study, the RTTOV model was configured for all-sky radiances with four widely recognized DDA shapes (block column, thinplate, sector snowflake and six-bullet rosette) and mie-sphere. The optical properties of hydrometeors are provided by mie-tables (pre-computed database) for each DDA shape.

This study was conducted for Vardah Cyclone over the Bay of Bengal during the winter season (6–12 December 2016) and its track is shown in Figure 12. The flow diagram in Figure 13 explains the simulation of AMSR-2 radiance using WRF forecasts and the RTTOV forward operator. The AMSR-2 observations are averaged to model resolution for comparison.

7.1 Results of observed and simulated Tb

Figure 14 shows the AMSR-2 band 13 observations (Fig. 14(a)) and simulated radiance with cloud ice mie-sphere, sector snowflake, six-bullet rosette, block column and thin-plate for the Vardah Cyclone (21240 samples). The simulated BT predicts the closest pattern as observed BT near the eye of the cyclone with all the DDA shapes. However, the BT inside the core is depressed due to the scattering that occurred from frozen snow particles. For the mie-sphere simulation, the lowest BT (255K) was much higher than the observed BT (124K) over the cloud and precipitation areas. But with DDA shapes, thin-plate was closely resembled with observation and block-column overestimated the lowest BT (Table 4) due to excess scattering at 89V in deep convective areas. The lack of frozen hydrometeor details in the Kain-Fritsch convection scheme also causes the model to deviate from the realistic simulations (Rysman *et al.*, 2016).

7.2 Results of sensitivity analysis to DDA shapes

This study used *h*-statistics (Eq. (9)) suggested by Geer and Baordo (2014) to measure the similarity between observed and simulated BTs in the statistical sense:

$$h = \frac{\left(\sum_{\text{bins}} \left| \log_{\# \text{observation}}^{\# \text{simulated}} \right| \right)}{\text{total no of bins}} \quad (9)$$

Here, the bin size is 2.5K.

Figure 15(a) shows the $\log_{\# \text{observation}}^{\# \text{simulated}}$ over the range of 120–280K BTs associated with mie-sphere and DDA shapes. Within the 120–200K bins, block column and thin-plate shapes have a positive log ratio, which means excessive occurrence of low BTs than observation, while six-bullet rosette and sector snowflake have a negative log ratio, indicating no occurrence of

BTs in this range. However, in the 210–280K bins, log ratio was almost zero, which indicates that simulated BTs were in good agreement with observations. The h values for each shape are given in Table 4; the smaller the number, the greater will be the similarity. The thin-plate shape shows lowest for this convective event.

Figure 15(b) shows the skewness of O-B values with mie-sphere and DDA shapes. Large negative or positive values indicate skew towards the left or right from the normal distribution curve. Thin-plate shapes have less positive value (+0.5) among the tested DDA shapes. Overall statistically, thin-plate shapes show optimum results for simulated BT over the Bay of Bengal region at band 13. However, Geer and Baordo (2014) stated that the sector snowflake has consistent results across all frequencies and the thin-plate shape always produces excessive scattering over the ocean. However, their study was done globally, while our analysis is for a single convective event (Vardah Cyclone); the finer spatial resolution (15 km *versus* 80 km) also reduces the representativity errors (Waller *et al.*, 2014).

7.3 Conclusion

In this case study we investigated the mie-sphere and DDA shapes for the accurate simulation of all-sky AMSR-2 radiances in RTTOV framework. The output from the WRF model forecasts, such as profiles of tempearture, humidity and hydrometeor, were given as input to the RTTOV model for the Vardah Cyclone. The h statistic and skewness analysis show that thin-plate shapes have the finest results among the four DDA shapes and mie-sphere over the Bay of Bengal. Adding grapuel and hail into the RTTOV model can improve the accuracy of all-sky simulation at higher frequency. Future work will be focused on assimilation of higher frequencies in WRF data assimilation for the prediction of deep convective events.

8 Prospects for the future

In this article, we discussed DA techniques, which receiving increased attention in hydrology and meteorology. The main focus in this review article was on EKF and EnKF techniques. Several challenges remain the field, which include, but are not limited to the following.

1. There is a lack of integration of research results into operational forecast systems (Liu *et al.*, 2012). Most of the literature focuses on synthetic tests, theoretical advances (e.g. Reichle *et al.*, 2008; Crow and Ryu , 2009; Kumar *et al.*, 2009) and the use of DA in distributed hydrological scenarios (Komma *et al.*, 2008; Clark *et al.*, 2008; Salamon and Feyen, 2009; Brocca *et al.*, 2010; Lee *et al.*, 2011, 2012; Yan and Moradkhani, 2016). Use of a distributed approach results in large dimensionality of the inverse problem which, in turn, causes overfitting in the updating stage of DA. In

spite of the advancements in DA techniques, operational practice relies on hydrological forecasting using lumped models (Seo et al., 2009; Chen et al., 2012). An exception is the system running in Meteo-France, which uses best linear unbiased estimator (BLUE) with streamflow observations for updating the soil moisture states within a distributed model.

2. There is a lack of consensus across the NWP community on the best approach to tackle model error. Palmer (2012) states that developing physical parameterizations directly in a probabilistic context shall be viable. When we move towards stochastic physical parameterizations, it would result in a substantial departure from popular model development practice leading to recalibration of model physics. The alternative approach might be to use multiphysics ensemble approaches (Candille 2009). Pennell and Reichler (2011) have shown that different models owing to their inherent limitations results in overconfident climate projection.
3. In DA studies, one can create a long list of additional error sources which may arise from, for instance, incorrectly specified observation error statistics (Frehlich 2006; Gorin and Tsyrlnikov 2011; Stewart et al. 2013). The efficiency of variational DA techniques is dictated by the background error covariance matrices, which are large matrices making it computationally difficult to explicitly state. The background statistics define how observations are spread in model space. An important feature of the EnKF is that covariance is being passed through assimilation cycles. The covariance obtained using EnKF will dictate the balance between error growth with model dynamics and error reduction by data assimilation (Houtekamer et al 2016). In the variational systems, covariances are obtained with the NMC method (Parrish and Derber 1992) which uses the difference between forecasts issued at two different times. Despite more than one decade of operational experience with the EnKF algorithm, there is a lack of reasonable and convincing algorithms to describe the system error. There is significant room for improvement in this area.

The case study examples show how new observations are revolutionizing prediction in hydrology and atmospheric sciences. With new data becoming increasingly available, the distinctions between modelling and field work may start to break down (McLaughlin 1995), with modellers becoming interested in extracting complementary information from field data and field hydrologists may learn more from datasets produced by model-based assimilation techniques.

Funding

The authors acknowledge the support from Indian Institute of Technology Bombay through the research grant 15IRCCSG016 and the support from the department of science and technology through the early career research project grant number 001559.

References

- Abaza, M., et al., (2014a). Sequential streamflow assimilation for short term hydrological ensemble forecasting. *Journal of Hydrology*, 519, 2692–2706. doi:10.1016/j.jhydrol.2014.08.038
- Abaza, M., Garneau, C., and Anctil, F., (2014b). Comparison of sequential and variational streamflow assimilation techniques for short-term hydrological forecasting. *Journal of Hydrologic Engineering*, 20 (2), 04014042.
- Abhilash, S., Sahai, A. K., Mohankumar, K., George, J. P. and Das, S. (2012). Assimilation of Doppler Weather Radar Radial Velocity and Reflectivity Observations in WRF-3DVAR System for Short-Range Forecasting of Convective Storms. *Pure and Applied Geophysics* 169(11), 2047–2070. doi:10.1007/s00024-012-0462-z
- Alpert, J. C. and Kumar, V. K. (2007). Radial wind super-obs from the WSR-88D radars in the NCEP operational assimilation system. *Monthly Weather Review*. 135(3), 1090–1109. doi:10.1175/MWR3324.1
- Alvarez-Garreton, C., et al. (2014). The impacts of assimilating satellite soil moisture into a rainfall-runoff model in a semi-arid catchment. *Journal of Hydrology*, 519, 2763–2774. doi:10.1016/j.jhydrol.2014.07.041
- Amezcuia, J., Goodliff, M. and Leeuwen, P. J. Van, (2017). A weak-constraint 4DEnsembleVar. Part I: Formulation and simple model experiments. *Tellus: Series A, Dynamic Meteorology and Oceanography*. 69(1). doi:10.1080/16000870.2016.1271564
- Anctil, F., Perrin, C., and Andreassian, V., (2003). ANN output updating of lumped conceptual rainfall/runoff forecasting models. *Journal of the American Water Resources Association*, 39 (5), 1269–1279. doi:10.1111/j.1752-1688.2003.tb03708.x

- Andreadis, K.M. and Lettenmaier, D.P., (2006). Assimilating remotely sensed snow observations into a macroscale hydrology model. *Advances in Water Resources*, 29 (6), 872–886. doi:10.1016/j.advwatres.2005.08.004
- Arpe, K., B. A. Hollingsworth, A. C. Lorenc, M. S. Tracton, G. Cats, S. Uppala, and P. Källberg , (1985) . The response of numerical weather prediction systems to fuge level iib data. Part I: Analyses, *Quarterly Journal of the Royal Meteorological Society*, 111(463), 1–66, doi:10.1002/qj.49711146302.3
- Ballard, S., M. Dixon, S. Swarbrick, Z. Li, O. Stiller, H. Lean, F. Rihan, and C. Collier, (2005). Assimilation of radar data in the Met Office mesoscale and convective scale forecast systems. Preprints, 32nd Conf. on Radar Meteorology/11th Conf. on Mesoscale Processes, Albuquerque, NM, Amer. Meteor. Soc., JP1J.9. [Available online at <http://ams.confex.com/ams/pdffiles/96499.pdf>.]
- Bannister, R. N. (2017). A review of operational methods of variational and ensemble-variational data assimilation. *Quarterly Journal of the Royal Meteorological Society*. 143(703), 607–633. doi:10.1002/qj.2982
- Barker, D. M., W. Huang, Y.-R. Guo, A. J. Bourgeois, and Q. N. Xiao., (2004). A Three-Dimensional Variational Data Assimilation System for MM5: Implementation and Initial Results, *Monthly Weather Review*, 132(4), 897–914, doi:10.1175/1520-0493(2004)132<0897:ATVDAS>2.0.CO;2.
- Barnes SL. (1964). A technique for maximizing details in numerical weather map analysis. *Journal of Applied Meteorology* 3, 396–409
- Bergthórsson, P. and Döös, B.R. (1955). Numerical Weather Map Analysis1. Tellus, 7, 329–340. doi:10.1111/j.2153-3490.1955.tb01170.x
- Bhowmik, S. K. R., and K. Prasad., (2001). Some characteristics of Limited-Area Model-Precipitation forecast of Indian monsoon and evaluation of associated flow features, *Meteorology and Atmospheric Physics*, 76, 223–236, doi:10.1007/s007030170031.
- Blankenship, C.B., Case, J.L., Crosson, W.L., Zavodsky, B.T., (2018). Correction of Forcing-Related Spatial Artifacts in a Land Surface Model by Satellite Soil Moisture Data Assimilation. *IEEE Geoscience and Remote Sensing Letters*. 15, 498–502. doi:10.1109/LGRS.2018.2805259
- Bowler, N.E., Clayton, A.M., Jardak, M., Jermey, P.M., Lorenc, A.C., Wlasak, M.A., Barker, D.M., Inverarity, G.W. and Swinbank, R. (2017). The effect of improved ensemble covariances on hybrid variational data assimilation. *Quarterly Journal of the Royal Meteorological Society*. 143, 785–797. doi:10.1002/qj.2964
- Bratseth, A.M. (1986). Statistical interpolation by means of successive corrections. Tellus A, 38A: 439-447. doi:10.1111/j.1600-0870.1986.tb00476.x
- Brocca, L., F. Melone, T. Moramarco, W. Wagner, V. Naeimi, Z. Bartalis, and S. Hasenauer (2010). Improving runoff prediction through the assimilation of the ASCAT soil moisture product, *Hydrology and Earth System Sciences*, 14(10), 1881–1893, doi:10.5194/hess-14-1881-2010.
- Brocca, L., et al. (2012). Assimilation of surface- and root-zone ASCAT soil moisture products into rainfall-runoff modeling. *IEEE Transactions on Geoscience and Remote Sensing*, 50 (7), 2542–2555. doi:10.1109/TGRS.2011.2177468
- Broersen, P.M.T., (2007). Error correction of rainfall-runoff models with the armasel program. *IEEE Transactions on Instrumentation and Measurement*, 56 (6), 2212–2219. doi:10.1109/TIM.2007.908252
- Buehner M. (2005). Ensemble-derived stationary and flow-dependent background-error covariances: evaluation in a quasi-operational NWP setting. *Quarterly Journal of the Royal Meteorological Society*. 131: 1013–1043.

- Candille, G., (2009). The Multiensemble Approach: The NAEFS Example. *Monthly Weather Review*, **137**, 1655–1665, <https://doi.org/10.1175/2008MWR2682.1>
- Caparrini, F., F. Castelli, and D. Entekhabi (2004a), Variational estimation of soil and vegetation turbulent transfer and heat flux parameters from sequences of multisensor imagery, *Water Resources Research*, **40**, W12515, doi:10.1029/2004WR003358
- Caparrini, F., F. Castelli, and D. Entekhabi (2004b), Estimation of surface turbulent fluxes through assimilation of radiometric surface temperature sequences, *Journal of Hydrometeorology*, **5**, 145–159, doi:[10.1175/1525-7541\(2004\)005<0145:EOSTFT>2.0.CO;2](https://doi.org/10.1175/1525-7541(2004)005<0145:EOSTFT>2.0.CO;2)
- Charney, J. G., and Drazin, P. G. (1961). Propagation of planetary-scale disturbances from the lower into the upper atmosphere, *Journal of Geophysical Research*, **66**(1), 83–109, doi:10.1029/JZ066i001p00083.
- Charney, J.G., Fjörtoft, R. And Von Neumann, J. (1950). Numerical Integration of the Barotropic Vorticity Equation. *Tellus*, **2**: 237-254. doi:10.1111/j.2153-3490.1950.tb00336.x
- Chen, H., et al. (2013). Hydrological data assimilation with the Ensemble Square-Root-Filter: Use of streamflow observations to update model states for real-time flash flood forecasting. *Advances in Water Resources*, **59**, 209–220. doi:10.1016/j.advwatres.2013.06.010
- Chen, J., W. Zhang, J. Gao, and K. Cao (2012), Assimilating multi-site measurements for semi-distributed hydrological model updating, *Quaternary International*, **282**, 122–129, doi:10.1016/j.quaint.2012.01.030
- Chen, F., et al. (2011). Improving hydrologic predictions of a catchment model via assimilation of surface soil moisture. *Advances in Water Resources*, **34** (4), 526–536. Doi:10.1016/j.advwatres.2011.01.011
- Clark, M.P., et al. (2008). Hydrological data assimilation with the ensemble Kalman filter: use of streamflow observations to update states in a distributed hydrological model. *Advances in Water Resources*, **31** (10), 1309–1324. doi:10.1016/j.advwatres.2008.06.005
- Clark, M.P., et al. (2006). Assimilation of snow covered area information into hydrologic and land-surface models. *Advances in Water Resources*, **29** (8), 1209–1221. doi:10.1016/j.advwatres.2005.10.001
- Cohn, S. E., and D. F. Parrish, (1991). The behavior of forecast error covariances for a Kalman filter in two dimensions. *Monthly Weather Review*, **119**, 1757–1785.
- Coustau, M., et al. (2013). Benefits and limitations of data assimilation for discharge forecasting using an event-based rainfall–runoff model. *Natural Hazards and Earth System Science*, **13** (3), 583–596. doi:10.5194/nhess-13-583-2013
- Cosgrove, B.A., et al. (2003). Real-time and retrospective forcing in the North American Land Data Assimilation System (NLDAS) project. *Journal of Geophysical Research: Atmospheres* (1984–2012), **108** (D22), 8842.
- Crow, R. T., Ryu, D., (2009) A new data assimilation approach for improving runoff prediction using remotely-sensed soil moisture retrievals, *Hydrology and Earth System Sciences*, **13** (1), pp. 1-16
- Crow, R. T., Wood, E. F., (2003), The assimilation of remotely sensed soil brightness temperature imagery into a land surface model using Ensemble Kalman filtering: a case study based on ESTAR measurements during SGP97, *Advances in Water Resources*, **26**(2), 137-149, doi: 10.1016/S0309-1708(02)00088-X.
- Cressman, G.P., (1959). An Operational Objective Analysis System. *Monthly Weather Review*, **87**, 367–374, [https://doi.org/10.1175/1520-0493\(1959\)087<0367:AOOAS>2.0.CO;2](https://doi.org/10.1175/1520-0493(1959)087<0367:AOOAS>2.0.CO;2)

- Daley, R., (1991). *Atmospheric Data Analysis*. Cambridge University Press, 457 pp.
- Das, A. K., U. C. Mohanty, S. Das, M. Mandal, and S. R. Kalsi (2003). Circulation characteristics of a monsoon depression during BOBMEX-99 using high-resolution analysis, *Journal of Earth System Science*, 112(2), 165–184, doi:10.1007/BF02701985.
- De Lannoy, Gabrielle J M, Reichle, Rolf H., Pauwels, V.R.N (2013a). Global Calibration of the GEOS-5 L-Band Microwave Radiative Transfer Model over Nonfrozen Land Using SMOS Observations. *Journal of Hydrometeorology*. 14, 765–785. Doi:10.1175/JHM-D-12-092.1
- De Lannoy, Gabrielle J M, Reichle, Rolf H (2013b) Global assimilation of Multiangle and Multipolarization SMOS Brightness Temperature Observations into GEOS-5 Catchment Land Surface Model for Soil Moisture Estimation. *Journal of Hydrometeorology*, 669-691. doi: 10.1175/JHM-D-15-0037.1
- De Lannoy, G. J. M., R. H. Reichle, K. R. Arsenault, P. R. Houser, S. Kumar, N. E. C. Verhoest, and V. R. N. Pauwels (2012), Multiscale assimilation of Advanced Microwave Scanning Radiometer-EOS snow water equivalent and Moderate Resolution Imaging Spectroradiometer snow cover fraction observations in northern Colorado, *Water Resources Research*, 48, W01522, doi:[10.1029/2011WR010588](https://doi.org/10.1029/2011WR010588).
- DeChant, C., and H. Moradkhani (2011), Radiance data assimilation for operational snow and streamflow forecasting, *Advances Water Resources*, 34(3), 351–364, doi:10.1016/j.advwatres.2010.12.009.
- Derber, J. C., D. F. Parrish, and S. J. Lord (1991) The new global operational analysis system at the national meteorological center. *Weather and Forecasting*, 6, 538-547
- Dong, J., J. P. Walker, P. R. Houser, and C. Sun (2007), Scanning multichannel microwave radiometer snow water equivalent assimilation, *Journal of Geophysical Research*, 112, D07108, doi:10.1029/2006JD007209
- Draper, C.S., Reichle, R.H., De Lannoy, G.J.M., Liu, Q (2012) Assimilation of passive and active microwave soil moisture retrievals. *Geophysical Research Letters*. 39, 1–5. Doi:10.1029/2011GL050655
- Draper, C., et al (2011) Assimilation of ASCAT near-surface soil moisture into the SIM hydrological model over France. *Hydrology and Earth System Sciences*, 15 (12), 3829–3841.
- Dudhia, J., (1989). Numerical Study of Convection Observed during the Winter Monsoon Experiment Using a Mesoscale Two-Dimensional Model. *Journal of the Atmospheric Sciences*, doi:10.1175/1520-0469(1989)046<3077:NSOCOD>2.0.CO;2
- Dunne, S., Entekhabi, D. (2005) An ensemble-based analysis approach to land data assimilation. *Water Resources Research*., 41, W02013, doi:10.1029/2004WR003449
- Durand, M., and S. A. Margulis (2007), Correcting first-order errors in snow water equivalent estimates using a multifrequency, multiscale radiometric data assimilation scheme, *Journal of Geophysical Research*, 112, D13121, doi:[10.1029/2006JD008067](https://doi.org/10.1029/2006JD008067).
- Durand, M., and S. A. Margulis (2007), Correcting first-order errors in snow water equivalent estimates using a multifrequency, multiscale radiometric data assimilation scheme, *Journal of Geophysical Research*, 112, D13121, doi:[10.1029/2006JD008067](https://doi.org/10.1029/2006JD008067).
- Ek, M.B., K.E., Mitchell, Y. Lin, E., Rogers, P. Grunmann, V. Koren, G. Gayno, J. D. Tarpley (2003). Implementation of Noah land surface model advances in the National Centres for Environmental Prediction operational mesoscale Eta Model. *Journal of Geophysical Research: Atmospheres*, 108(D22), 8851, doi:10.1029/2002JD003296
- Emrouznejad, A. (2016). Big Data Optimization: Recent Developments and Challenges, *Springer International publishing*, vol. 18.
- Entekhabi, D., Njoku, E. G., P. E. O'Neill, K. H. Kellogg, W. T. Crow, W. N. Edelstein, J. K. Entin, S. D. Goodman, T. J. Jackson, J. Johnson, J. Kimball, J. R. Piepmeier, R. D.

- Koster, N. Martin, K. C. McDonald, M. Moghaddam et. al., (2010) The soil moisture active passive (SMAP) mission, in Proceedings of the IEEE, 98, 704-716, doi: 10.1109/JPROC.2010.2043918
- Evensen, G. (1994) Sequential data assimilation with a nonlinear quasigeostrophic model using Monte Carlo methods to forecast error statistics. *Journal of Geophysical Research: Oceans* (1978–2012), 99 (C5), 10143–10162. doi:10.1029/94JC00572
- Eyre, J.R., Kelly, G.A., McNally A.P., Andersson, E. and Persson A., (1993). Assimilation of TOVS radiance information through one-dimensional variational analysis. *Quarterly Journal of the Royal Meteorological Society*, 119, 1427-1463.
- Fang H., Liang S. & Gerrit Hoogenboom (2011) Integration of MODIS LAI and vegetation index products with the CSM–CERES–Maize model for corn yield estimation, International Journal of Remote Sensing, 32:4, 1039-1065, DOI: 10.1080/01431160903505310
- Figa-Saldana, J., J. Wilson, E. Attema, R. Gelsthorpe, M. R., Drinkwater, A. Stoffelen (2002) The Advanced scatterometer (ASCAT) on the meteorological operational (metop) Platform: A follow on for European wind scatterometers. *Canadian Journal of Remote Sensing*. 28, 404-412, doi:10.5589/m02-035
- Fletcher, S.J., G.E. Liston, C.A. Hiemstra, and S.D. Miller, (2012) Assimilating MODIS and AMSR-E Snow Observations in a Snow Evolution Model. *Journal of Hydrometeorology*, 13, 1475–1492, <https://doi.org/10.1175/JHM-D-11-082.1>
- Frehlich, R., (2006). Adaptive data assimilation including the effect of spatial variations in observation error. *Quarterly Journal of Royal Meteorological Society*. 132, 1225–1257, doi:<https://doi.org/10.1256/qj.05.146>.
- Ganesh, S., Pradhan, A., & Indu, J. (2019). Evaluation of GPM sampling error over major basins in Indian subcontinent using bootstrap technique. *Advances in Space Research*, 63, 3289-3302.
- Gandin. L. S. (1966). Objective analysis of meteorological fields. *Quarterly Journal of the Royal Meteorological Society*. 92, 447, doi:[10.1002/qj.49709239320](https://doi.org/10.1002/qj.49709239320)
- Geer, A.J, Bauer, P., (2011). Observation errors in all-sky data assimilation. *Quarterly Journal of the Royal Meteorological Society*, 137, 2024-2037, doi:10.1002/qj.830.
- Geer, A.J., (2013). All-sky assimilation: better snow-scattering radiative transfer and addition of SSMIS humidity sounding channels. Technical Memorandum, 706, ECMWF, Reading, UK, available from <http://www.ecmwf.int>.
- Geer, A.J., Baordo, F., (2014). Improved scattering radiative transfer for frozen hydrometeors at microwave frequencies. *Atmospheric Measurement Techniques*, 7, 1839–1860. doi: 10.5194/amt-7-1839-2014
- Geer, A.J., Bauer, P., English, S.J. (2012). Assimilating AMSU-A temperature sounding channels in the presence of cloud and precipitation. Technical Memorandum, 670, ECMWF, Reading, UK, available from <http://www.ecmwf.int>.
- Geer, A.J., Lonitz, K., Weston, P., Kazumori, M., Okamoto, K., Zhu, Y., Liu, E.H., Collard, A., Bell, W., Migliorini, S., Chambon, P., Fourrie, N., Kim, M.J., Watts, C.K., Schraff, C. (2018). All-sky satellite data assimilation at operational weather forecasting centres. *Quarterly Journal of the Royal Meteorological Society*, 144, 1191-1217.
- Ghil, M., (1989) Meteorological data assimilation for oceanographers. Part I: Description and theoretical framework, *Dynamics of Atmospheres and Oceans*, 13 (3-4), 171-218.
- Ghosh, S., Karmakar, S., Saha, A., Mohanty, M. P., Ali, S., Raju, S. K., Krishnakumar, V., et al. (2019). Development of India's First Integrated Expert Urban Flood Forecasting System for the City of Chennai. *Current Science*. 117(5), 741–745.
- Gilchrist, B. And Cressman, G.P. (1954). An Experiment in Objective Analysis. *Tellus*, 6: 309-318. doi:10.1111/j.2153-3490.1954.tb01126.x

- Govindankutty, M., a. Chandrasekar, a. K. Bohra, J. P. George, and M. Das Gupta (2008) The Impact of Assimilation of MODIS Observations Using WRF-VAR for the Prediction of a Monsoon Depression During September 2006, *The Open Atmospheric Science Journal*, 2(1), 68–78, doi:10.2174/1874282300802010068.
- Gorin, V. E., and M. D. Tsyrulnikov, (2011). Estimation of multivariate observation-error statistics for AMSU-A data. *Monthly Weather Review*, 139, 3765–3780, doi:<https://doi.org/10.1175/2011MWR3554.1>.
- Guerbette, J., Mahfouf, J.F., Plu, M., (2016). Towards the assimilation of all-sky microwave radiances from the SAPHIR humidity sounder in a limited area NWP model over tropical regions. *Tellus A: Dynamic Meteorology and Oceanography*, 68. doi:10.3402/tellusa.v68.28620
- Gustafsson, N. (2007). Discussion on ‘4D-Var or EnKF?’, *Tellus A: Dynamic Meteorology and Oceanography*, 59, 5, 774-777, DOI: 10.1111/j.1600-0870.2007.00262.x
- Hamill, T.M. and C. Snyder, (2000). A Hybrid Ensemble Kalman Filter–3D Variational Analysis Scheme. *Monthly Weather Review*, 128, 2905–2919, doi:[https://doi.org/10.1175/1520-0493\(2000\)128<2905:AHEKFV>2.0.CO;2](https://doi.org/10.1175/1520-0493(2000)128<2905:AHEKFV>2.0.CO;2)
- Han, X., H.-J. H. Franssen, R. Rosolem, R. Jin, X. Li, and H. Vereecken (2015). Correction of systematic model forcing bias of CLM using assimilation of cosmic-ray Neutrons and land surface temperature: A study in the Heihe Catchment, China, *Hydrology and Earth System Sciences*, 19, 615–629.
- Han, E., Merwade, V., Heathman, G. C., (2012). Implementation of surface soil moisture data assimilation with watershed scale distributed hydrological model, *Journal of Hydrology*, 416-417, 98-117, doi: 10.1016/j.jhydrol.2011.11.039.
- Hind, O., Gejadze, I., Malaterre, P-O., Franck, M., (2018a) River discharge estimation from synthetic SWOT-type observations using variational data assimilation and full Saint-Venant hydraulic model. *Journal of Hydrology*, 559, 638-647.
- Hind, O., Gejadze, I., Malaterre, P.-O., Durand, M., Wei, R., Frasson, R. P. M., et al. (2018b). Discharge estimation in ungauged basins through variational data assimilation: The potential of the SWOT mission. *Water Resources Research*, 54, 2405– 2423.
- Hocking, J., Rayer, P., Rundle, D., Saunders, R., Matricardi, M., Geer, A., Brunel, P., Vidot, J (2017) “RTTOV v12 Users Guide”, NWCSAF report. EUMETSAT: Darmstadt, Germany.
- Hoke, J. E. & Anthes, R. A. (1976). The Initialization of Numerical Models by a Dynamic-Initialization Technique. *Monthly Weather Review*. 104, 1551–1556 doi:10.1175/1520-0493(1976)104<1551:TIONMB>2.0.CO;2
- Hong, G., Heygster, G., Miao, J., Kunzi, K., (2005). Detection of tropical deep convective clouds from AMSU-B water vapor channels measurements. *Journal of Geophysical Research: Atmospheres*, 110, 1–15. doi:10.1029/2004JD004949
- Hong, S.-Y., Noh, Y., Dudhia, J (2006). A New Vertical Diffusion Package with an Explicit Treatment of Entrainment Processes. *Monthly Weather Review*. 134, 2318–2341. doi:10.1175/MWR3199.1
- Hong, S., Lim, J., (2006). The WRF single-moment 6-class microphysics scheme (WSM6). *Journal of the Korean Meteorological Society*, 42, 2, 129-151.
- Hu, M., Xue, M., Gao, J. & Brewster, K. (2006). 3DVAR and Cloud Analysis with WSR-88D Level-II Data for the Prediction of the Fort Worth, Texas, Tornadic Thunderstorms. Part II: Impact of Radial Velocity Analysis via 3DVAR. *Monthly Weather Review*. 134(2), 699–721. doi:10.1175/MWR3093.1
- Huffman, G. J., Bolvin, D. T. & Nelkin, E. J. (2017). Integrated Multi-satellitE Retrievals for GPM (IMERG) Technical Documentation. NASA GSFC, 47, [Available online at http://pmm.nasa.gov/sites/default/files/document_files/IMERG_doc.pdf.]

- Houser, P. R., Shuttleworth, W. J., Famiglietti, J. S., Gupta, H. V., Syed, K. H., and Goodrich, D. C. (1998). Integration of soil moisture remote sensing and hydrologic modeling using data assimilation, *Water Resources Research*, 34(12), 3405–3420, doi:10.1029/1998WR900001.
- Houser, P.R., De Lannoy, G.J., and Walker, J.P., (2005). Hydrologic data assimilation. In: A. Aswathanarayana, ed. *Advances in Water Science Methodologies*. The Netherlands: AA Balkema, p. 230.
- Houtekamer, P.L. and F. Zhang, (2016). Review of the Ensemble Kalman Filter for Atmospheric Data Assimilation. *Monthly Weather Review*, 144, 4489–4532, <https://doi.org/10.1175/MWR-D-15-0440.1>
- Ide, K., M. Ide Ghil, and a C. Lorenc (1997). Unified Notation for Data Assimilation : Operational, sequential, and variational. *Journal of the Meteorological Society of Japan*, 75, 181-189.
- Indu. J and D. Nagesh Kumar (2016). Rainfall Screening Methodology using TRMM Data over a River Basin, *Hydrological Sciences Journal*, 61,14, 2540–2551 doi: 10.1080/02626667.2015.1133908.
- Indu. J and D. Nagesh Kumar (2015). Evaluation of Precipitation Retrievals from Orbital Data Products of TRMM of TRMM over a Subtropical basin in India, *IEEE Transactions on Geoscience and Remote Sensing*, 53, 12, 6429–6442, doi:10.1109/TGRS.2015.2440338,
- Indu. J and D. Nagesh Kumar (2014a). Evaluation of TRMM PR Sampling Error over a Subtropical Basin using Bootstrap Technique, *IEEE Transactions on Geoscience and Remote Sensing*, 52, 11, 6870 - 6881, doi:10.1109/TGRS.2014.2304466.
- Indu. J and D. Nagesh Kumar (2014b) Copula based Modeling of TRMM TMI Brightness Temperature with Rainfall Type, *IEEE Transactions on Geoscience and Remote Sensing*, IEEE, 52, 8, 4832-4845, August 2014, doi:10.1109/TGRS.2013.2285225.
- Ines, A.V.M., Das, N.N., Hansen, J.W., Njoku, E.G., (2013). Assimilation of remotely sensed soil moisture and vegetation with crop simulation model for maize yield prediction, *Remote Sensing of Environment*, 138, 149-164, doi: 10.1016/j.rse.2013.07.018.
- Irmak, A., and B. Kamble (2009). Evapotranspiration data assimilation with genetic algorithms and SWAP model for on-demand irrigation, *Irrigation Science*, 28(1), 101–112, doi:10.1007/s00271-009-0193-9.
- JAXA (Japan Aerospace Exploration Agency). (2013). Data User's Manual for the Advanced Microwave Scanning Radiometer 2 (AMSR2) onboard the Global Change Observation Mission 1st –Water “SHIZUKU” 2nd Edition, Available at http://suzaku.eorc.jaxa.jp/GCOM_W/data/doc/amr2_data_user_guide.pdf
- Jianfeng, G., Xiao, Q., Kuo, Y.-H., Barker, D.M., Jishan, X., Xiaoxing, M., (2005) Assimilation and simulation of typhoon Rusa (2002) using the WRF system. *Advances in Atmospheric Sciences*, 22, 415–427. <https://doi.org/10.1007/BF02918755>
- Kain, J.S., (2004). The Kain–Fritsch Convective Parameterization: An Update. *Journal of Applied Meteorology*, 43, 170–181.
- Kaheil, Y.H., Gill, M.K., McKee, M., Bastidas, L.A., Rosero, E., (2008). Downscaling and assimilation of surface soil moisture using ground truth measurements. *Geoscience and remote sensing. Transactions on IEEE* 46 (5), 1375–1384.
- Kalnay, E. (2003) Atmospheric Modeling, Data Assimilation, and Predictability. Cambridge, UK: Cambridge University Press, 341.
- Kalnay, E, Hong Li, Takemasa Miyoshi, Shu-Chih Yang & Joaquim Ballabrera-Poy, (2007). 4-D-Var or ensemble Kalman filter?, *Tellus A: Dynamic Meteorology and Oceanography*, 59:5, 758-773, DOI: 10.1111/j.1600-0870.2007.00261.x
- Kazumori, M., English, S.J., (2015). Use of the ocean surface wind direction signal in

- microwave radiance assimilation. *Quarterly Journal of the Royal Meteorological Society*, 141, 1354–1375. doi:10.1002/qj.2445
- Kazumori, M., Geer, A.J., English, S.J., (2014). Effects of all-sky assimilation of GCOM-W1/AMSR2 radiances in the ECMWF system. Technical Memorandum, 732, ECMWF, Reading, UK, available from <http://www.ecmwf.int>.
- Kerr, Y. H., P. Waldteufel, J. P. Wigneron, S. Delwart, F. Cabot, J. Boutin, M. R. Escorihuela, J. Font, N. Reul, C. Gruhier, S. E. Juglea, M. R. Drinkwater, A. Hahne, M-N. Manuel, M. Susanne (2010) The SMOS Mission: New tool for monitoring key elements of the global water cycle. *Proceedings of the IEEE*. 98, 666-687, doi: 10.1109/JPROC.2010.2013032
- Komma, J., G. Blöschl, and C. Reszler (2008), Soil moisture updating by ensemble Kalman filtering in real-time flood forecasting, *Journal of Hydrology.*, 357(3–4), 228– 242.
- Koster, R. D., and Coauthors, (2006) GLACE: The Global Land–Atmosphere Coupling Experiment. Part I: Overview. *Journal of Hydrometeorology.*, 7, 590–610.
- Kuchment, L. S. and Romanov, P. and Gelfan, A. N. and Demidov, V. N. (2010). Use of satellite-derived data for characterization of snow cover and simulation of snowmelt runoff through a distributed physically based model of runoff generation. *Hydrology and Earth System Sciences*. 14, 339-350, doi:10.5194/hess-14-339-2010
- Kumar, S. V., Reichle, R. H., Peters-Lidard, C. D., Koster, R. D., Zhan, X., Crow, W. T., et al (2008) A land surface data assimilation framework using the land information system: Description and applications. *Advances in Water Resources*. 31 (11), 1419– 1432, doi: 10.1016/j.advwatres.2008.01.013.
- Kumar, S. V., Peters-Lidard, C. D., Santenello, J. A., Reichle, R. H., Draper, C. S., Koster, R. D., et al (2015) Evaluating the utility of satellite soil moisture retrievals over irrigated areas and the ability of land data assimilation methods to correct for unmodeled processes. *Hydrology and Earth System Sciences.*, 19(11), 4463–4478, doi: 10.5194/hess-19-4463-2015
- Kumar, S. V., C. D. Peters-Lidard, D. M. Mocko, et al. (2014). Assimilation of passive microwave-based soil moisture and snow depth retrievals for drought estimation. *Journal of Hydrometeorology.*, 15 (6): 2446-2469,doi: 10.1175/JHM-D-13-0132.1
- Kunkee, D.B., Poe, G.A., Boucher, D.J., Swadley, S.D., Hong, Y., Wessel, J.E., Uliana, E.A., (2008). Design and evaluation of the first special sensor microwave imager/sounder. *IEEE Transactions on Geoscience and Remote Sensing*, 46, 863–883. <https://doi.org/10.1109/TGRS.2008.917980>
- Kummerow, C., Barnes, W., Kozu, T., Shiue, J., Simpson, J., (1998). The Tropical Rainfall Measuring Mission (TRMM) sensor package. *Journal of Atmospheric and Ocean Technology*, 15, 809–817.
- Lecomte, P., and W. Wagner, ERS wind scatterometer commissioning and in-flight calibration (1998), *Proceedings of Workshop on Emerging Scatterometer Applications: From Research to Operations, Emerging Scatterometer Applications-SP-424*. 261– 270.
- Lee, H., D.-J. Seo, and V. Koren (2011), Assimilation of streamflow and in situ soil moisture data into operational distributed hydrologic models: Effects of uncertainties in the data and initial model soil moisture states, *Advances Water Resources*, 34(12), 1597–1615, doi:10.1016/j.advwatres.2011.08.012
- Lee, H., D.-J. Seo, Y. Liu, V. Koren, P. McKee, and R. Corby (2012), Variational assimilation of streamflow into operational distributed hydrologic models: Effect of spatiotemporal scale of adjustment, *Hydrology and Earth System Sciences*, 16(7), 2233–2251, doi:10.5194/hess-16-2233-2012.

- Lettenmaier, D. P. (2017), Observational breakthroughs lead the way to improved hydrological predictions, *Water Resources Research*, 53, 2591–2597, doi:10.1002/2017WR020896.
- Leisenring, M. and Moradkhani, H. (2011), Snow water equivalent prediction using Bayesian data assimilation methods, *Stochastic Environmental Research and Risk Assessment*, 25, 1–18.
- Li, Z., and I. M. Navon (2001) Optimality of variational data assimilation and its relationship with the Kalman filter and smoother, *Quarterly Journal of the Royal Meteorological Society*, 127, 661–883.
- Li, Y., D. Ryu, A. W. Western, and Q. Wang (2015), Assimilation of stream discharge for flood forecasting: Updating a semidistributed model with an integrated data assimilation scheme, *Water Resources Research*, 51, 3238–3258, doi:10.1002/2014WR016667.
- Liston, G. E., (1999) Interrelationships among snow distribution, snowmelt, and snow cover depletion: Implications for atmospheric, hydrologic, and ecologic modeling. *Journal of Applied Meteorology*, 38, 1474–1487.
- Liston, G.E. and C.A. Hiemstra, (2008). A Simple Data Assimilation System for Complex Snow Distributions (SnowAssim). *Journal of Hydrometeorology*, 9, 989–1004, <https://doi.org/10.1175/2008JHM871.1>
- Lievens, H., Al Bitar, A., Verhoest, N.E.C., Cabot, F., De Lannoy, G.J.M., Drusch, M., Dumedah, G., Hendricks Franssen, H.-J., Kerr, Y., Tomer, S.K., Martens, B., Merlin, O., Pan, M., van den Berg, M.J., Vereecken, H., Walker, J.P., Wood, E.F., Pauwels, V.R.N (2015a) Optimization of a Radiative Transfer Forward Operator for Simulating SMOS Brightness Temperatures over the Upper Mississippi Basin. *Journal of Hydrometeorology*, 16, 1109–1134. doi:10.1175/JHM-D-14-0052.1
- Lievens, H., De Lannoy, G.J.M., Al Bitar, A., Drusch, M., Dumedah, G., Hendricks Franssen, H.J., Kerr, Y.H., Tomer, S.K., Martens, B., Merlin, O., Pan, M., Roundy, J.K., Vereecken, H., Walker, J.P., Wood, E.F., Verhoest, N.E.C., Pauwels, V.R.N (2015b) Assimilation of SMOS soil moisture and brightness temperature products into a land surface model. *Remote Sensing of Environment*, 180, 292–304. doi:10.1016/j.rse.2015.10.033
- Liu, C., E.J. Zipser, D.J. Cecil, S.W. Nesbitt, and S. Sherwood, (2008). A Cloud and Precipitation Feature Database from Nine Years of TRMM Observations. *Journal of Applied Meteorology and Climatology*., 47, 2712–2728, doi.org/10.1175/2008JAMC1890.1
- Liu, C., Q. Xiao, and B. Wang, (2008). An Ensemble-Based Four-Dimensional Variational Data Assimilation Scheme. Part I: Technical Formulation and Preliminary Test. *Monthly Weather Review*., 136, 3363–3373, <https://doi.org/10.1175/2008MWR2312.1>
- Liu, G., (2008). A database of microwave single-scattering properties for nonspherical ice particles. *Bulletin of the American Meteorological Society*, 89, 1563–1570. doi:10.1175/2008BAMS2486.1
- Liu, C., Q. Xiao, and B. Wang, (2009). An Ensemble-Based Four-Dimensional Variational Data Assimilation Scheme. Part II: Observing System Simulation Experiments with Advanced Research WRF (ARW). *Monthly Weather Review*, 137, 1687–1704, <https://doi.org/10.1175/2008MWR2699.1>
- Liu, Y., et al. (2012) Advancing data assimilation in operational hydrologic forecasting: progresses, challenges, and emerging opportunities. *Hydrology and Earth System Sciences*, 16 (10), 3863–3887. doi:10.5194/hess-16-3863-2012

- Liu, Y. And Gupta, H.V (2007) Uncertainty in hydrologic modeling: Toward an integrated data assimilation framework. *Water Resources Research*, 43, 7. doi:10.1029/2006WR005756
- Lorenc, A. C. (2017). Improving ensemble covariances in hybrid variational data assimilation without increasing ensemble size. . *Quarterly Journal of the Royal Meteorological Society*. 143(703), 1062–1072. doi:10.1002/qj.2990
- Lorenc, A. C. (1981), A global three-dimensional multivariate statistical interpolation scheme,*Monthly Weather Review*,109: 701–721.
- Mahrt, L., Ek, M (1984) The Influence of Atmospheric Stability on Potential Evaporation. *Journal of Applied Meteorology and Climatology*, doi:10.1175/1520-0450(1984)023<0222:TIOASO>2.0.CO;2
- Mandal, M., U. C. Mohanty, and A. K. Das (2006) Impact of satellite derived wind in mesoscale simulation of Orissa super cyclone, Indian *Journal of Geo-Marine Sciences*, 35(2), 161–173.
- Mangla, R., J. Indu and V. Lakshmi (2020) Evaluation of convective storms using spaceborne radars over Indo-Gangetic Plains and Western Coast of India, *Meteorological Applications*, doi: 10.1002/met.1917.
- Margulis, S. A., mclaughlin, D., Entekhabi, D., & Dunne, S (2002) Land data assimilation and estimation of soil moisture using measurements from the Southern Great Plains 1997 Field Experiment. *Water Resources Research*, 38, 1299
- Massari, C., et al. (2014) Potential of soil moisture observations in flood modelling: estimating initial conditions and correcting rainfall. *Advances in Water Resources*, 74, 44–53. doi:10.1016/j.advwatres.2014.08.004
- Mazzoleni, M., L. Alfonso, J. Chacon-Hurtado, and D. Solomatine (2015), Assimilating uncertain, dynamic and intermittent streamflow observations in hydrological models, *Advances in Water Resources*, 83, 323–339, doi:10.1016/j.advwatres.2015.07.004.
- Mclaughlin, D. (1995) Recent developments in hydrologic data assimilation. *Reviews of Geophysics*, 33 (S2), 977–984. doi:10.1029/95RG00740
- McNally A, Watt P., (2003). A cloud detection algorithm for high spectral resolution infrared sounders. *Quarterly Journal of the Royal Meteorological Society*, 129, 3411-3423.
- Mcmillan, H., et al. (2013) Operational hydrological data assimilation with the recursive ensemble Kalman filter. *Hydrology and Earth System Sciences*, 17 (1), 21–38. doi:10.5194/hess-17-21-2013
- Meng, C. L., Li, Z.-L., Zhan, X., Shi, J. C., and Liu, C. Y. (2009), Land surface temperature data assimilation and its impact on evapotranspiration estimates from the Common Land Model, *Water Resources Research*, 45, W02421, doi:10.1029/2008WR006971.
- Mitchell, K.E., et al. (2004) The multi-institution North American Land Data Assimilation System (NLDAS): Utilizing multiple GCIP products and partners in a continental distributed hydrological modeling system. *Journal of Geophysical Research: Atmospheres* (1984–2012), 109 (D7). doi:10.1029/2003JD003823
- Mlawer, E.J., Taubman, S.J., Brown, P.D., Iacono, M.J., Clough, S.A., (1997). Radiative transfer for inhomogeneous atmospheres: RRTM, a validated correlated-k model for the longwave. *Journal of Geophysical Research: Atmospheres*, 102, 16663–16682. doi:10.1029/97JD00237
- Montzka C, Pauwels VRN, Franssen H-JH, Han X, Vereecken H. (2012). Multivariate and Multiscale Data Assimilation in Terrestrial Systems: A Review. *Sensors*. 12(12), 16291-16333.
- Moradkhani, H. (2008) Hydrologic remote sensing and land surface data assimilation. *Sensors*, 8 (5), 2986–3004. doi:10.3390/s8052986

- Moradkhani, H., DeChant, C. M., and Sorooshian, S. (2012), Evolution of ensemble data assimilation for uncertainty quantification using the particle filter-Markov chain Monte Carlo method, *Water Resources Research*, 48, W12520, doi:[10.1029/2012WR012144](https://doi.org/10.1029/2012WR012144).
- Munier, S., Polebitski, A., Brown, C., Belaud, G., and Lettenmaier, D. P. (2015), SWOT data assimilation for operational reservoir management on the upper Niger River Basin, *Water Resources Research*, 51, 554– 575, doi:[10.1002/2014WR016157](https://doi.org/10.1002/2014WR016157).
- Mukhopadhyay, P., J. Sanjay, W. R. Cotton, and S. S. Singh (2005) Impact of surface meteorological observations on RAMS forecast of monsoon weather systems over the Indian region, *Meteorology and Atmospheric Physics*, 108, 77–108, doi:[10.1007/s00703-004-0090-y](https://doi.org/10.1007/s00703-004-0090-y).
- Nair, A. S., Indu, J., (2019). Improvement of land surface model simulations over India via data assimilation of satellite-based soil moisture products, *Journal of Hydrology*, 573, 406-421
- Nair, A.S., Indu, J., (2018). A Coupled Land Surface and Radiative Transfer Models based on relief correction for a reliable land data assimilation over mountainous terrain. *IEEE Geoscience and Remote Sensing Letters*, 15 (11), 1657-1661
- Nair, A. S., Indu, J., (2017). Performance Assessment of Multi Source Weighted Ensemble Precipitation (MSWEP) product over India, Climate, Special Issue on Using Tropical Rainfall Measuring Mission (TRMM) Data in Research and Applications, *Climate*, 5(1), doi:[10.3390/cli5010002](https://doi.org/10.3390/cli5010002);
- Nair, A.S., Indu, J., (2016). Enhancing Noah Land Surface Model Prediction Skill over Indian Subcontinent by Assimilating SMOPS Blended Soil Moisture. *Remote Sensing*, 8(12),976, doi:[10.3390/rs8120976](https://doi.org/10.3390/rs8120976)
- Njoku, E. G., T. J. Jackson, V. Lakshmi, T. K. Chan, S. V. Nghiem (2003) Soil Moisture retrieval from AMSR-E, *IEEE Transactions on Geoscience and Remote Sensing*, 41, 215-227
- Noh, S. J., Y. Tachikawa, M. Shiiba, and S. Kim (2013), Ensemble Kalman filtering and particle filtering in a lag-time window for short-term streamflow forecasting with a distributed hydrologic model, *Journal of Hydrologic Engineering*, 18(12), 1684–1696, doi:[10.1061/\(ASCE\)HE.1943-5584.0000751](https://doi.org/10.1061/(ASCE)HE.1943-5584.0000751)
- Noh, S. J., O. Rakovec, A. H. Weerts, and Y. Tachikawa (2014), On noise specification in data assimilation schemes for improved flood forecasting using distributed hydrological models, *Journal of Hydrology*, 519, 2707–2721, doi:[10.1016/j.jhydrol.2014.07.049](https://doi.org/10.1016/j.jhydrol.2014.07.049).
- Okamoto, K., (2017). Evaluation of IR radiance simulation for all-sky assimilation of Himawari-8/AHI in a mesoscale NWP system. *Quarterly Journal of the Royal Meteorological Society*. 143, 1517–1527. <https://doi.org/10.1002/qj.3022>.
- Osuri, K. K., Mohanty, U. C., Routray, A. & Niyogi, D. (2015). Improved Prediction of Bay of Bengal Tropical Cyclones through Assimilation of Doppler Weather Radar Observations. *Monthly Weather Review*, 143(11), 4533–4560. doi:[10.1175/MWR-D-13-00381.1](https://doi.org/10.1175/MWR-D-13-00381.1)
- Palmer T (2012) Towards the probabilistic earth-system simulator: a vision for the future of climate and weather prediction. *Quarterly Journal of the Royal Meteorological Society*, 138(665):841–861
- Parajka, J. and Naeimi, V. and Bloschl, G. and Wagner, W. and Merz, R. and Scipal, K. (2006). Assimilating scatterometer soil moisture data into conceptual hydrologic models at the regional scale, *Hydrology and Earth System Sciences*, 10 (3), 353-368
- Parajka, J. And Blöschl, G (2008) The value of MODIS snow cover data in validating and calibrating conceptual hydrologic models. *Journal of Hydrology*, 358 (3–4), 240–258. Doi:[10.1016/j.jhydrol.2008.06.006](https://doi.org/10.1016/j.jhydrol.2008.06.006)

- Pan, M., et al (2003) Snow process modeling in the North American Land Data Assimilation System (NLDAS): 2. Evaluation of model simulated snow water equivalent. *Journal of Geophysical Research: Atmospheres* (1984–2012), 108 (D22). doi:10.1029/2003JD003994
- Pan, H. -L., & Mahrt, L. (1987) Interaction between soil hydrology and boundary-layer development. *Boundary-Layer Meteorology*, 38, 185-202
- Pan, M., E. F. Wood, R. Wójcik, and M. F. McCabe (2008), Estimation of regional terrestrial water cycle using multi-sensor remote sensing observations and data assimilation, *Remote Sensing of Environment*, 112(4), 1282–1294, doi:[10.1016/j.rse.2007.02.039](https://doi.org/10.1016/j.rse.2007.02.039).
- Pan, M., Sahoo, A.K., Wood, E.F., Al Bitar, A., Leroux, D., Kerr, Y.H. (2012) An initial assessment of SMOS derived soil moisture over the continental United States. *IEEE Journal of Selected Topics in Applied Earth Observations and Remote Sensing*, 5, 1448–1457. doi:10.1109/JSTARS.2012.2194477
- Panofsky, R.A., 1949. Objective Weather-Map Analysis. *Journal of Meteorology*, 6, 386–392, [https://doi.org/10.1175/1520-0469\(1949\)006<0386:OWMA>2.0.CO;2](https://doi.org/10.1175/1520-0469(1949)006<0386:OWMA>2.0.CO;2)
- Parrish, D.F. and J.C. Derber, (1992). The National Meteorological Center's Spectral Statistical-Interpolation Analysis System. *Monthly Weather Review*, 120, 1747–1763, [https://doi.org/10.1175/1520-0493\(1992\)120<1747:TNCSS>2.0.CO;2](https://doi.org/10.1175/1520-0493(1992)120<1747:TNCSS>2.0.CO;2)
- Parrish, M. A., Moradkhani, H., and DeChant, C. M. (2012), Toward reduction of model uncertainty: Integration of Bayesian model averaging and data assimilation, *Water Resources Research*, 48, W03519, doi:10.1029/2011WR011116.
- Pauwels, V.R.N. and De Lannoy, G.J.M. (2006) Improvement of modeled soil wetness conditions and turbulent fluxes through the assimilation of observed discharge. *Journal of Hydrometeorology*, 7 (3), 458–477. doi:10.1175/JHM490.1
- Pennell, C., and T. Reichler (2011), On the effective number of climate models, *Journal of Climate*, 24(9), 2358–2367, doi:10.1175/2010JCLI3814.1.
- Pipunic, R.C., J.P. Walker, A. Western (2008) Assimilation of remotely sensed data for improved latent and sensible heat flux prediction: a comparative synthetic study, *Remote Sensing of Environment*, 112 (4) (2008), pp. 1295-1305, doi:[10.1016/j.rse.2007.02.038](https://doi.org/10.1016/j.rse.2007.02.038)
- Pradhan A., Indu J. (2019) Uncertainty in Calibration of Variable Infiltration Capacity Model. In: Singh S., Dhanya C. (eds) Hydrology in a Changing World. Springer Water. Springer, Cham
- Pulliainen, J. (2006), Mapping of snow water equivalent and snow depth in the boreal and sub-arctic zones by assimilating space-borne microwave radiometer data and ground-based observations, *Remote Sensing of Environment*, 101, 257– 269.
- Qin, C.; Jia, Y.; Su, Z.; Zhou, Z.; Qiu, Y.; Suhui, S. (2008), Integrating Remote Sensing Information Into A Distributed Hydrological Model for Improving Water Budget Predictions in Large-scale Basins through Data Assimilation. *Sensors*, 8, 4441-4465
- Rafieeininasab, A., D.-J. Seo, H. Lee, and S. Kim (2014), Comparative evaluation of maximum likelihood ensemble filter and ensemble Kalman filter for real-time assimilation of streamflow data into operational hydrologic models, *Journal of Hydrology*, 519, 2663–2675, doi:10.1016/j.jhydrol.2014.06.052
- Rajan D, Mitra AK, Rizvi SRH, Paliwal RK, Bohra AK, Bhatia VB (2001). Impact of satellite derived moisture in a global numerical weather prediction model. *Atmosfera*., 14, 203–209.
- Rakovec, O., et al. (2015). Operational aspects of asynchronous filtering for hydrological forecasting. *Hydrology and Earth System Sciences Discussions*, 12 (3), 3169–3203. doi:10.5194/hessd-12-3169-2015

- Reichle, R. H., D. B. McLaughlin, D. Entekhabi, (2002a). Hydrologic data assimilation with ensemble kalman filter, *Monthly Weather Review*, 130, 103-114
- Reichle, R. H., J. P. Walker, R. D. Koster, and P. R. Houser (2002b). Extended versus ensemble kalman filtering for land data assimilation, *Journal of Hydrometeorology*, 3, 728-740
- Reichle, R. H., & Koster, R. D (2003). Assessing the impact of horizontal error correlations in background fields on soil moisture estimation. *Journal of Hydrometeorology*, 4, 1229-1242
- Reichle, R. H., and Koster, R. D. (2004), Bias reduction in short records of satellite soil moisture, *Geophysical Research Letters*, 31, L19501, doi:10.1029/2004GL020938.
- Reichle, R.H., Koster, R.D. (2005) Global assimilation of satellite surface soil moisture retrievals into the NASA catchment land surface model. *Geophysical Research Letters*. 32, 1–4. doi:10.1029/2004GL021700
- Reichle, R.H. (2008) Data assimilation methods in the Earth sciences. *Advances in Water Resources*, 31 (11), 1411–1418. doi:10.1016/j.advwatres.2008.01.001
- Reichle, R.H., S.V. Kumar, S.P. Mahanama, R.D. Koster, and Q. Liu, (2010) Assimilation of Satellite-Derived Skin Temperature Observations into Land Surface Models. *Journal of Hydrometeorology*, 11, 1103–1122, <https://doi.org/10.1175/2010JHM1262.1>
- Renard, B., D. Kavetski, G. Kuczera, M. Thyre, and S. Franks, (2010). Understanding predictive uncertainty in hydrologic modeling. The challenge of identifying input and structural errors. *Water Resources Research*, 46, W05521, doi:<https://doi.org/10.1029/2009WR008328>.
- Richardson, L. F. (1922). Weather prediction by numerical process Cambridge University Press, *Quarterly Journal of the Royal Meteorological Society*, 48: 282-284. doi:10.1002/qj.49704820311
- Roberts, N. M. (2005). An investigation of the ability of a storm scale configuration of the Met Office NWP model to predict flood producing rainfall, Met Office Technical Report 455, 80.
- Roberts, N. M., and H. W. Lean (2008). Scale-Selective Verification of Rainfall Accumulations from High-Resolution Forecasts of Convective Events, *Monthly Weather Review*, 136(1), 78–97, doi:10.1175/2007MWR2123.1.
- Rodell, M., P. R. Houser, A. A. Berg, J. S. Famiglietti (2005). Evaluation of 10 methods for initializing a land surface model, *Journal of Hydrometeorology*, 6, 146-155,
- Rodell, M. And Houser, P (2004). Updating a land surface model with MODIS-derived snow cover. *Journal of Hydrometeorology*, 5 (6), 1064–1075. doi:10.1175/JHM-395.1
- Rodell, M., Houser, R. P., Jambor, A.U.E., Gottschalck, J (2004). The global land data assimilation system. *Bulletin of the American Meteorological Society*, 3, 381-394, doi: 10.1175/BAMS-85-3-381
- Routray, A., Mohanty, U.C., Osuri, K.K., Kar, S.C., Niyogi, D., (2016). Impact of Satellite Radiance Data on Simulations of Bay of Bengal Tropical Cyclones Using the WRF-3DVAR Modeling System. *IEEE Transactions on Geoscience and Remote Sensing*, 54, 2285–2303. doi:10.1109/TGRS.2015.2498971
- Routray, A., U. C. Mohanty, A. K. Das, and N. V Sam (2005). Study of heavy rainfall event over West Coast of India using analysis nudging in MM5 during ARMEX-I, *Mausam*, 1(January), 107–120.
- Routray, A., U. C. Mohanty, D. Niyogi, S. R. H. Rizvi, and K. K. Osuri (2010). Simulation of heavy rainfall events over Indian monsoon region using WRF-3DVAR data assimilation system, *Meteorology and Atmospheric Physics*, 106(1-2), 107–125, doi:10.1007/s00703-009-0054-3.

- Routray, A., Mohanty, U. C., Osuri, K. K. & Kiran Prasad, S. (2013). Improvement of Monsoon Depressions Forecast with Assimilation of Indian DWR Data Using WRF-3DVAR Analysis System. *Pure and Applied Geophysics*. 170(12), 2329–2350. doi:10.1007/s00024-013-0648-z
- Rysman, J.-F., Berthou, S., Claud, C., Drobinski, P., Chaboureau, J.-P., Delanoë, J., (2016). Potential of microwave observations for the evaluation of rainfall and convection in a regional climate model in the frame of hymex and MED-CORDEX. *Climate Dynamics*, doi:10.1007/s00382-016-3203-7
- Sahoo, A.K., et al. (2013). Assimilation and downscaling of satellite observed soil moisture over the Little River Experimental Watershed in Georgia, USA. *Advances in Water Resources*, 52, 19–33. Doi:10.1016/j.advwatres.2012.08.007
- Salamon, P., and L. Feyen (2009). Assessing parameter, precipitation, and predictive uncertainty in a distributed hydrological model using sequential data assimilation with the particle filter, *Journal of Hydrology*, 376(3), 428–442.
- Samuel, J., et al., (2014). Assessing model state and forecasts variation in hydrologic data assimilation. *Journal of Hydrology*, 513, 127–141. doi:10.1016/j.jhydrol.2014.03.048
- Sandeep, S., A. Chandrasekar, and D. Singh (2006). The impact of assimilation of AMSU data for the prediction of a tropical cyclone over India using a mesoscale model, *International Journal of Remote Sensing*, 27(20), 4621–4653, doi:10.1080/01431160600857410.
- Saunders, R., Hocking, J., Rundle, D., Rayer, P., Havemann, S., Matricardi, M., Geer, A., Lupu, C., Brunel, P., Vidot, J., (2017). RTTOV-12 science and validation report. Technical Report, NWPSAF, verion 1.0, Doc ID: NWPSAF-MO-TV-41
- Santanello, J. A., S. V. Kumar, C. D. Peters-Lidard, P. M. Lawston (2016). Impact of soil moisture assimilation on land surface model spin-up and coupled land-atmosphere prediction. *Journal of Hydrometeorology*, 17, 517-540, doi: 10.1175/JHM-D-15-0072.1
- Schuurmans, M., P.A. Troch, A.A. Veldhuizen, W.G.M. Bastiaanssen, M.F.P. Bierkens (2003). Assimilation of remotely sensed latent heat flux in a distributed hydrological model, *Advances in Water Resources*, 26 (2) (2003), pp. 151-159, doi: 10.1016/s0309-1708(02)00089-1
- Scipal, K., et al. (2005). Soil moisture-runoff relation at the catchment scale as observed with coarse resolution microwave remote sensing, *Hydrology and Earth System Sciences*, 9, 173 – 183.
- Seo, D.-J., Koren, V., and Cajina, N. (2003). Real-time variational assimilation of hydrologic and hydrometeorological data into operational hydrologic forecasting. *Journal of Hydrometeorology*, 4 (3), 627–641. doi:10.1175/1525-7541(2003)004<0627:RVAOHA>2.0.CO;2
- Seo, D.-J., L. Cajina, R. Corby, and T. Howieson (2009), Automatic state updating for operational streamflow forecasting via variational data assimilation, *Journal of Hydrology*, 367(3), 255–275, doi:10.1016/j.jhydrol.2009.01.019.
- Sheffield, J., et al. (2003). Snow process modeling in the North American Land Data Assimilation System (NLDAS): 1. Evaluation of model simulated snow cover extent. *Journal of Geophysical Research: Atmospheres*, (1984–2012), 108 (D22). doi:10.1029/2002JD003274
- Singh, R., Ojha, S.P., Kishtawal, C.M., Pal, P.K., Kiran Kumar, A.S., (2016). Impact of the assimilation of INSAT-3D radiances on short-range weather forecasts. *Quarterly Journal of the Royal Meteorological Society*, 142, 120–131. doi: 10.1002/qj.2636
- Sini, F., Boni, G., Caparrini, F., and Entekhabi, D. (2008), Estimation of large-scale evaporation fields based on assimilation of remotely sensed land temperature, *Water Resources Research*, 44, W06410, doi:10.1029/2006WR005574.

- Skamarock, W.C., Klemp, J.B., Dudhi, J., Gill, D.O., Barker, D.M., Duda, M.G., Huang, X.-Y., Wang, W., Powers, J.G., 2008. A Description of the Advanced Research WRF Version 3. Technical Report, 113. doi:10.5065/D6DZ069T
- Slater, A. G. and Clark, M. P. (2006). Snow data assimilation via an ensemble Kalman filter, *Journal of Hydrometeorology*, 7, 478–493.
- Stauffer, D. R., & Seaman, N. L. (1990). Use of four-dimensional data assimilation in a limited-area mesoscale model. Part I: experiments with synoptic-scale data. *Monthly Weather Review*, 118(6), 1250-1277. [https://doi.org/10.1175/1520-0493\(1990\)118<1250:UOFDDA>2.0.CO;2](https://doi.org/10.1175/1520-0493(1990)118<1250:UOFDDA>2.0.CO;2)
- Steward, J.L., Navon, I.M., Zupanski, M. and Karmitsa, N. (2012). Impact of non-smooth observation operators on variational and sequential data assimilation for a limited-area shallow-water equation model *Quarterly Journal of the Royal Meteorological Society*, 138, 323-339. doi:10.1002/qj.935
- Stewart, L. M., S. L. Dance, and N. K. Nichols, (2013). Data assimilation with correlated observation errors: Experiments with a 1-D shallow water model, *Tellus*, 65A, 19546, doi:<https://doi.org/10.3402/tellusa.v65i0.19546>.
- Sun, J., S. B. Trier, Q. Xiao, M. L. Weisman, H. Wang, Z. Ying, M. Xu, and Y. Zhang (2012). Sensitivity of 0–12-h Warm-Season Precipitation Forecasts over the Central United States to Model Initialization, *Weather Forecast.*, 27(4), 832–855, doi:10.1175/WAF-D-11-00075.1.
- Subramani, D., R. Chandrasekar, K. S. Ramanujam, and C. Balaji (2014). A new ensemble-based data assimilation algorithm to improve track prediction of tropical cyclones, *Natural Hazards*, 71(1), 659–682, doi:10.1007/s11069-013-0942-1.
- Tewari, M., Chen, F., Wang, W., Dudhia, J., Lemone, M.A., Mitchell, K., Ek, M., Gayno, G., Wegiel, J., Cuenca, R.H. (2004). Implementation and verification of the unified Noah land surface model in the WRF model. *Bulletin of the American Meteorological Society*, 2165–2170. doi: 10.1007/s11269-013-0452-7
- Thirel, G., E. Martin, J.-F. Mahfouf, S. Massart, S. Ricci, and F. Habets (2010a), A past discharges assimilation system for ensemble streamflow forecasts over France—Part 1: Description and validation of the assimilation system, *Hydrology and Earth System Sciences*, 14, 1623–1637, doi:10.5194/hess-14-1623-2010
- Thirel, G., E. Martin, J.-F. Mahfouf, S. Massart, S. Ricci, F. Regimbeau, and F. Habets (2010b), A past discharge assimilation system for ensemble streamflow forecasts over France—Part 2: Impact on the ensemble streamflow forecasts, *Hydrology and Earth System Sciences*, 14, 1639–1653, doi: 10.5194/hess-14-1639-2010
- Thiruvengadam, P., Indu, J. & Ghosh, S. (2019). Assimilation of Doppler Weather Radar data with a regional WRF-3DVAR system: Impact of control variables on forecasts of a heavy rainfall case. *Advances in Water Resources*. 126, 24-39. doi:10.1016/j.advwatres.2019.02.004
- Thiruvengadam, P., Indu, J., & Ghosh, S. (2020). Improving convective precipitation forecasts using ensemble-based background error covariance in 3DVAR radar assimilation system. *Earth and Space Science*, 7, e2019EA000667. <https://doi.org/10.1029/2019EA000667>
- Tian, X., Xie, Z., and Dai, A. (2008). An ensemble-based explicit four-dimensional variational assimilation method, *Journal of Geophysical Research*, 113, D21124, doi:10.1029/2008JD010358.
- Tian, X., Z. Xie, A. Dai, B. Jia, and C. Shi (2010). A microwave land data assimilation system: Scheme and preliminary evaluation over China. *Journal of Geophysical Research Atmospheres*, 115, 1-13, doi:10.1029/2010JD014370
- Tian, X. and Xie, Z. (2012). Implementations of a square-root ensemble analysis and a hybrid

- localisation into the POD-based ensemble 4DVar. *Tellus Series A: Dynamic Meteorology and Oceanography* 64(1), 18375. doi:10.3402/tellusa.v64i0.1837
- Tian, X. and Feng, X. (2015). A non-linear least squares enhanced POD-4DVar algorithm for data assimilation. *Tellus Series A: Dynamic Meteorology and Oceanography*. 67(1), 25340. doi:10.3402/tellusa.v67.25340
- Tong, W., G. Li, J. Sun, X. Tang, and Y. Zhang, (2016). Design Strategies of an Hourly Update 3DVAR Data Assimilation System for Improved Convective Forecasting. *Weather and Forecasting*, 31, 1673–1695, <https://doi.org/10.1175/WAF-D-16-0041.1>
- Tewari, M., Chen, F., Wang, W., Dudhia, J., lemone, M.A., Mitchell, K., Ek, M., Gayno, G., Wegiel, J., Cuenca, R.H. (2004). Implementation and verification of the unified Noah land surface model in the WRF model. *Bulletin of the American Meteorological Society*, 2165–2170. doi: 10.1007/s11269-013-0452-7
- Trudel, M., Leconte, R., and Paniconi, C (2014). Analysis of the hydrological response of a distributed physically-based model using postassimilation (enkf) diagnostics of streamflow and in situ soil moisture observations. *Journal of Hydrology*, 514, 192–201. doi:10.1016/j.jhydrol.2014.03.072
- Tauchi, T., Takeuchi, Y and Sato, Y., (2004). Assimilation of the Aqua/AMSR-E data to numerical weather predictions. *Proceedings of Geoscience and Remote Sensing Symposium, IGARSS '04 , IEEE International*, Vol 5, IEEE Operations Center, Piscataway, NJ, pp. 3199-3202.
- Vaidya, S. S., P. Mukhopadhyay, D. K. Trivedi, J. Sanjay, and S. S. Singh. (2004). Prediction of tropical systems over Indian region using mesoscale model, *Meteorology and Atmospheric Physics* , 72, 63–72, doi:10.1007/s00703-003-0019-x.
- Velpuri, N. M. G.B. Senay, R.K. Singh, S. Bohms, J.P. Verdin (2013). A comprehensive evaluation of two MODIS evapotranspiration products over the conterminous United States: using point and gridded FLUXNET and water balance ET. *Remote Sensing of Environment*, 139 (2013), pp. 35-49, doi:10.1016/j.rse.2013.07.013
- Vereecken, H., et al. (2015) Soil hydrology: recent methodological advances, challenges, and perspectives. *Water Resources Research*, 51 (4), 2616–2633. doi:10.1002/2014WR016852
- Verhoef, W. And Bach, H. (2003) Remote sensing data assimilation using coupled radiative transfer models. *Physics and Chemistry of the Earth, Parts A/B/C*, 28 (1–3), 3–13. doi:10.1016/S1474-7065(03)00003-2
- Vinodkumar, A. Chandrasekar, D. Niyogi, and K. Alapaty (2009). Impact of land surface representation and surface data assimilation on the simulation of an off-shore trough over the Arabian Sea, *Global and Planetary Change*, 67(1–2), 104–116, doi:10.1016/j.gloplacha.2008.12.004.
- Vinodkumar, A. Chandrasekar, K. Alapaty, and D. Niyogi (2008). The impacts of indirect soil moisture assimilation and direct surface temperature and humidity assimilation on a mesoscale model simulation of an Indian monsoon depression, *Journal of Applied Meteorology and Climatology*, 47(5), 1393–1412, doi:10.1175/2007JAMC1599.1.
- Vinodkumar, A. Chandrasekar, K. Alapaty, and D. Niyogi (2009). Assessment of data assimilation approaches for the simulation of a monsoon depression over the Indian monsoon region, *Boundary-Layer Meteorology.*, 133(3), 343–366, doi:10.1007/s10546-009-9426-y.
- Vinodkumar, A. Chandrasekar, K. Alapaty, and D. S. Niyogi (2007). The effect of a surface data assimilation technique and the traditional four-dimensional data assimilation on the simulation of a monsoon depression over India using a mesoscale model, *Natural Hazards*, 42(2), 439–453, doi:10.1007/s11069-006-9080-3.

- Vrugt, J. A., Clark, M. P., Diks, C. G. H., Duan, Q., and Robinson, B. A. (2006). Multi-objective calibration of forecast ensembles using Bayesian model averaging, *Geophysical Research Letters*, 33, L19817, doi:10.1029/2006GL027126.
- Vrugt, J. A., Cajo J.F. ter Braak, Cees G.H. Diks, Gerrit Schoups, (2013). Hydrologic data assimilation using particle Markov chain Monte Carlo simulation, *Advances in Water Resources*, 51, 457-478
- Waller, J.A., Dance, S.L., Lawless, A.S., Nichols, N.K., Eyre, J.R. (2014). Representativity error for temperature and humidity using the Met Office high-resolution model. *Quarterly Journal of the Royal Meteorological Society*, 140, 1189–1197. doi:10.1002/qj.2207.
- Waller, J.A., Dance, S.L., Nichols, N.K., (2016). Diagnosing Horizontal and Inter-Channel Observation Error Correlations for SEVIRI Observations using Observation-minus-Background and Observation-minus-Analysis statistics. *Remote Sensing*. 8. <https://doi.org/10.3390/rs8070581>.
- Wanders, N., et al. (2014). The benefits of using remotely sensed soil moisture in parameter identification of large-scale hydrological models. *Water Resources Research*, 50 (8), 6874–6891. doi:10.1002/wrcr.v50.8
- Wang, B., Liu, J., Wang, S., Cheng, W., Juan, L., Liu, C., Xiao, Q., et al. (2010). An economical approach to four-dimensional variational data assimilation. *Advances in Atmospheric Sciences*. 27(4), 715–727. doi:10.1007/s00376-009-9122-3
- Wang, H., Sun, J., Fan, S. & Huang, X.-Y. (2012). Indirect Assimilation of Radar Reflectivity with WRF 3D-Var and Its Impact on Prediction of Four Summertime Convective Events. *Journal of Applied Meteorology and Climatology*. 52(4), 889–902. American Meteorological Society. doi:10.1175/JAMC-D-12-0120.1
- Wang, W., Chau, K., Xu, D. et al. (2015). Improving Forecasting Accuracy of Annual Runoff Time Series Using ARIMA Based on EEMD Decomposition. *Water Resources Management*, 29, 2655–2675. <https://doi.org/10.1007/s11269-015-0962-6>
- Walker, J.P., Houser, P.R., and Reichle, R.H. (2003). New technologies require advances in hydrologic data assimilation. *EOS, Transactions, American Geophysical Union*, 84 (49), 545–551. doi:10.1029/2003EO490002
- Weerts, A. H., and G. Y. H. El Serafy (2006). Particle filtering and ensemble Kalman filtering for state updating with hydrological conceptual rainfall-runoff models, *Water Resources Research*, 42, W09403, doi:10.1029/2005WR004093.
- Xavier, V. F., A. Chandrasekar, H. Rahman, D. Niyogi, and K. Alapaty (2008). The effect of satellite and conventional meteorological data assimilation on the mesoscale modeling of monsoon depressions over India, *Meteorology and Atmospheric Physics*, 101(1–2), 65–92, doi:10.1007/s00703-008-0314-7.
- Xiao, Q., Kuo, Y.-H., Sun, J., Lee, W.-C., Lim, E., Guo, Y.-R. & Barker, D. M. (2005). Assimilation of Doppler Radar Observations with a Regional 3DVAR System: Impact of Doppler Velocities on Forecasts of a Heavy Rainfall Case. *Journal of Applied Meteorology*. 44(6), 768–788. doi:10.1175/JAM2248.1
- Xiao, Q., Lim, E., Won, D. J., Sun, J., Lee, W. C., Lee, M. S., Lee, W. J., et al. (2008). Doppler radar data assimilation in KMS's operational forecasting. *Bulletin of American Meteorological Society*. 89(1), 39–43. doi:10.1175/BAMS-89-1-39
- Xie, X., Zhang, D. (2010). Data assimilation for distributed hydrological catchment modeling via ensemble Kalman filter, *Advances in Water Resources*, 33 (6) (2010), pp. 678-690, doi:10.1016/j.advwatres.2010.03.012
- Xu, T., Bateni, S.M., Liang, S., Entekhabi, D., Mao, K., (2014). Estimation of surface turbulent heat fluxes via variational assimilation of sequences of land surface temperatures from geostationary operational environmental satellites, *Journal of*

- Geophysical Research: Atmospheres*, 119 (18) (2014), pp. 10780-10798, doi:10.1002/2014jd021814
- Xu, Q. (1996). Generalized Adjoint for Physical Processes with Parameterized Discontinuities. Part I: Basic Issues and Heuristic Examples. *Journal of Atmospheric Sciences*. 53(8), 1123–1142. American Meteorological Society. doi:10.1175/1520-0469(1996)053<1123:GAFPPW>2.0.CO;2
- Yan, H., and H. Moradkhani (2016), Combined assimilation of streamflow and satellite soil moisture with the particle filter and geostatistical modeling, *Advances in Water Resources*, 94, 364–378, doi:10.1016/j.advwatres.2016.06.002
- Yan, H., C. M. DeChant and H. Moradkhani, (2015). Improving Soil Moisture Profile Prediction With the Particle Filter-Markov Chain Monte Carlo Method, *IEEE Transactions on Geoscience and Remote Sensing*, vol. 53, no. 11, pp. 6134-6147.
- Yang, C., Liu, Z., Bresch, J., Rizvi, S.R.H., Huang, X.Y., Min, J., (2016). AMSR2 all-sky radiance assimilation and its impact on the analysis and forecast of Hurricane Sandy with a limited-area data assimilation system. *Tellus A: Dynamic Meteorology and Oceanography*, 68. doi:10.3402/tellusa.v68.30917
- Yang, K., Zhu, L., Chen, Y., Zhao, L., Qin, J., Lu, H., Tang, W., Han, M., Ding, B., Fang, N. (2015). Land Surface model calibration through microwave data assimilation for improving soil moisture simulations. *Journal of Hydrology*, 533, 266–276, doi: 10.1016/j.jhydrol.2015.12.018
- Yang, Y., Qiu, C. J. & Gong, J. D. (2006). Physical initialization applied in WRF-Var for assimilation of Doppler radar data. *Geophysical Research Letters*. 33(22), 2–7. doi:10.1029/2006GL027656
- Yin, J., Zhan, C., Ye, W., (2016). An experimental study on evapotranspiration data assimilation based on the hydrological model. *Water Resources Management*, 30 (14), pp. 5263-5279, doi:10.1007/s11269-016-1485-5
- Yu, P.-S. And Chen, S.-T. (2005) Updating real-time flood forecasting using a fuzzy rule-based model. *Hydrological Sciences Journal*, 50 (2), 265–278. doi:10.1623/hysj.50.2.265.61796
- Zhang, F., Zhang, M. & Hansen, J. A. (2009) Coupling ensemble Kalman filter with four-dimensional variational data assimilation. *Advances Atmospheric Sciences*. 26(1), 1–8. doi:10.1007/s00376-009-0001-8
- Zhan, X., Liu, J., Zhao, L., & Jensen, K (2011) *Soil moisture operational product system (SMOPS) algorithm theoretical basis document*. [Http://www.ospo.noaa.gov/Products/land/smops/documents.html](http://www.ospo.noaa.gov/Products/land/smops/documents.html).
- Zhang, X., X. Y. Huang, and N. Pan, (2013) Development of upgraded tangent linear and adjoint of the weather research and forecasting (WRF) model, *Journal of Atmospheric and Oceanic Technology*, 30(6), 1180–1188, doi:10.1175/JTECH-D-12-0021
- Zou, X. (1997), Tangent linear and adjoint of “on-off” processes and their feasibility for use in 4-dimensional variational data assimilation, *Tellus A: Dynamic Meteorology and Oceanography*, 49:1, 3-31, DOI: 10.3402/tellusa.v49i1.12209
- Zhou, S., Liu, W., Lin, W., (2017). The ratio of transpiration to evapotranspiration in a rainfed maize field on the Loess Plateau of China. *Water Supply*; 17 (1): 221–228. doi: <https://doi.org/10.2166/ws.2016.108>

Figure captions

Figure 1. Schematic representation of ensemble Kalman filter assimilation approach.

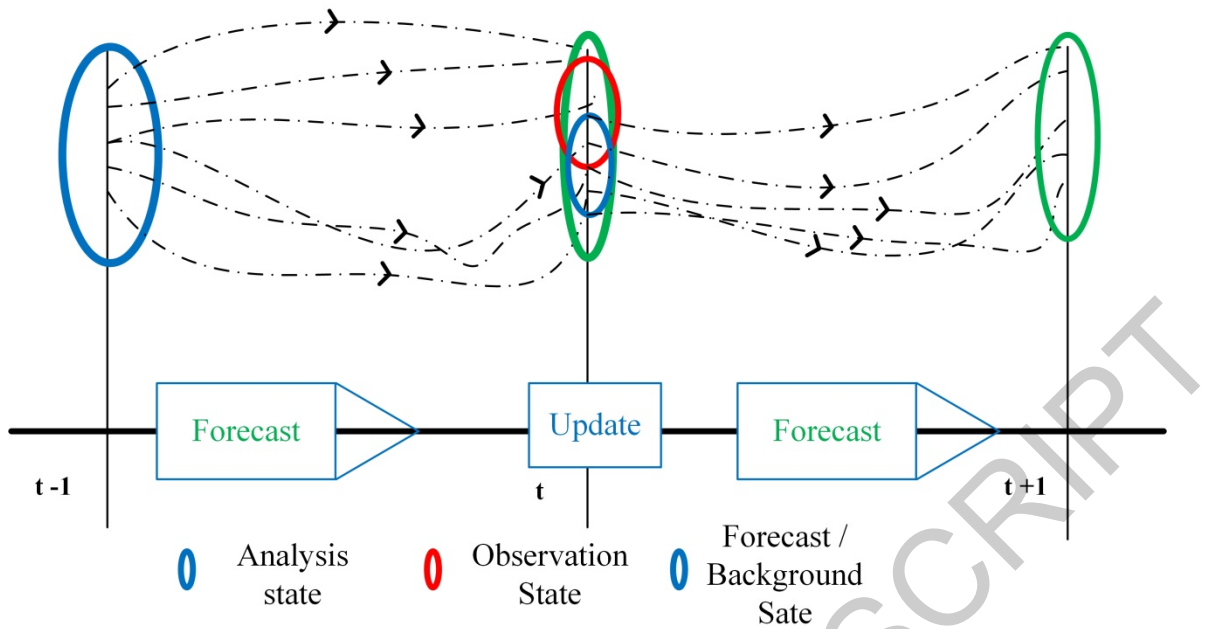


Figure 2. Study domain with inset location of *in situ* ISMN soil moisture network over the Central Tibetan Plateau.

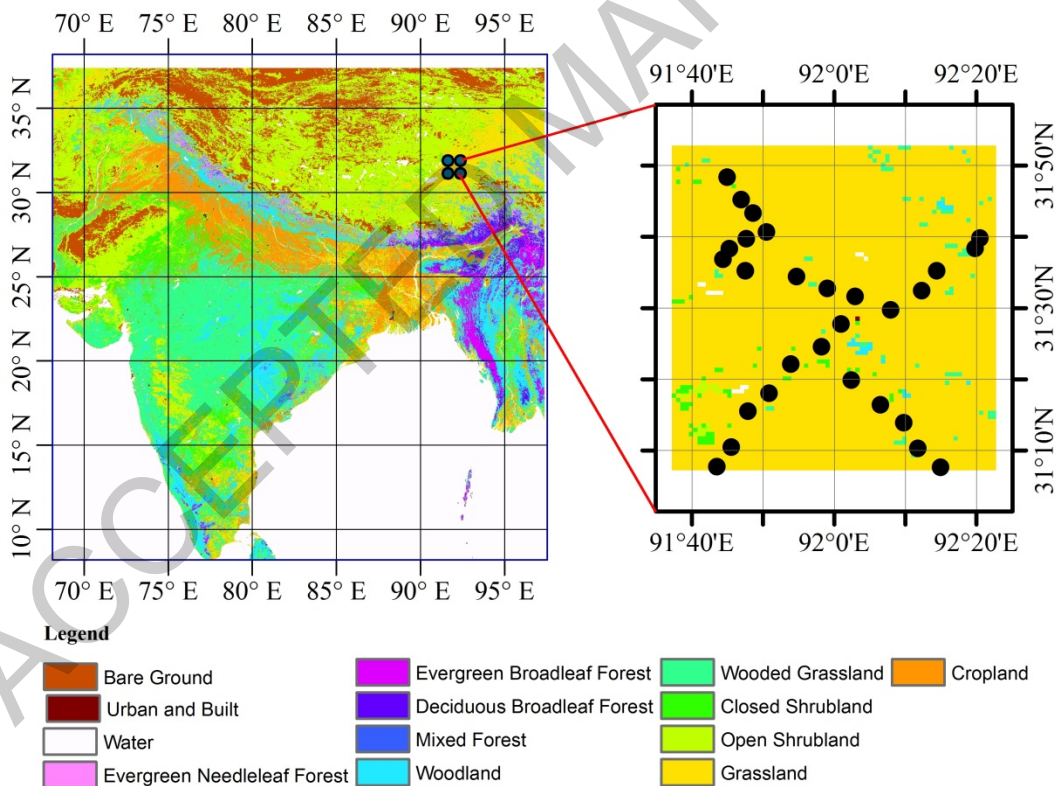


Figure 3. (a) and (c) Monthly mean of innovation over loop 1 (L-1), loop 2 (L-2), loop 3 (L-3) and loop 4 (L-4) for 2009 and 2010, respectively. (b) and (d) Yearly mean of innovation over loops L-1 to L-4 for 2009 and 2010, respectively.

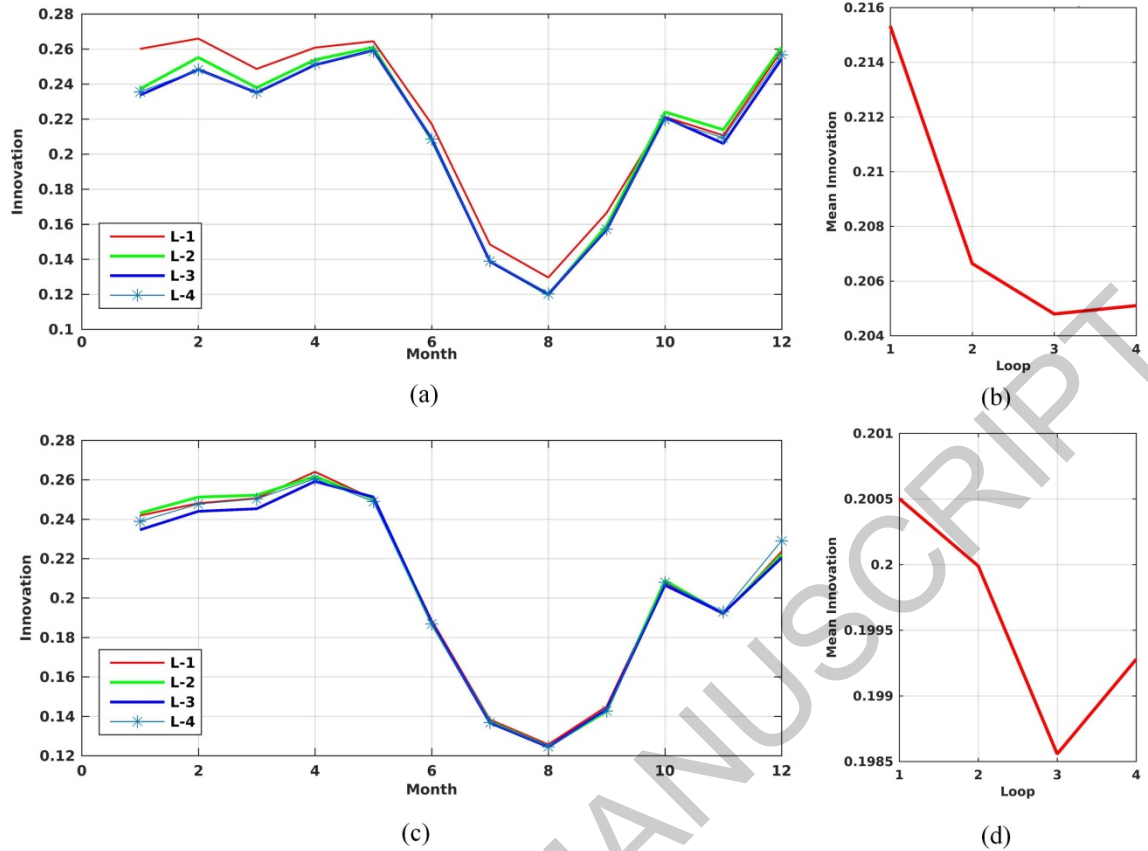


Figure 4. Variation of daily soil moisture in 2009–2010: (a) layer 1 from spin-up loop 1; (b) layer 1 from spin-up loop 4; (c) layer 2 from spin-up loop 1; (d) layer 2 from spin-up loop 4; (e) layer 3 from spin-up loop 1; (f) layer 3 from spin-up loop 4; (g) layer 4 from spin-up loop 1; (h) layer 4 from spin-up loop 4. OL: open loop, i.e. without assimilation; DA: data assimilation; OA-DA: difference between them.

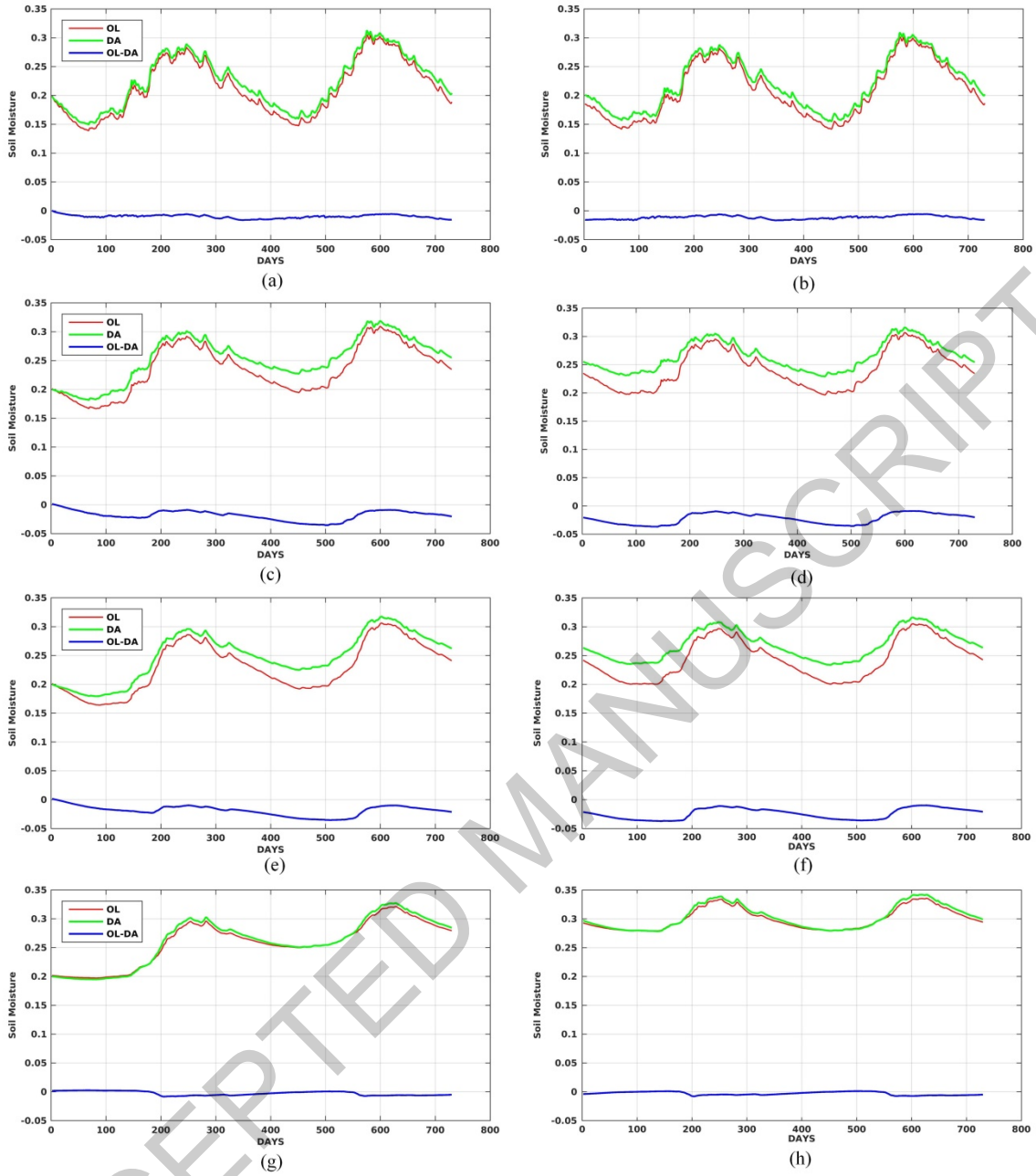


Figure 5. Yearly mean soil moisture for (a)–(d): layer 1, layer 2, layer 3 and layer 4 soil moisture, respectively, from OL (without assimilation) for 2009; (e)–(h) layer 1, layer 2, layer 3 and layer 4 soil moisture, respectively, with DA (data assimilation) for 2009. Similarly, (i)–(l) simulation with OL for 2010; (m)–(p) simulation with DA for 2010.

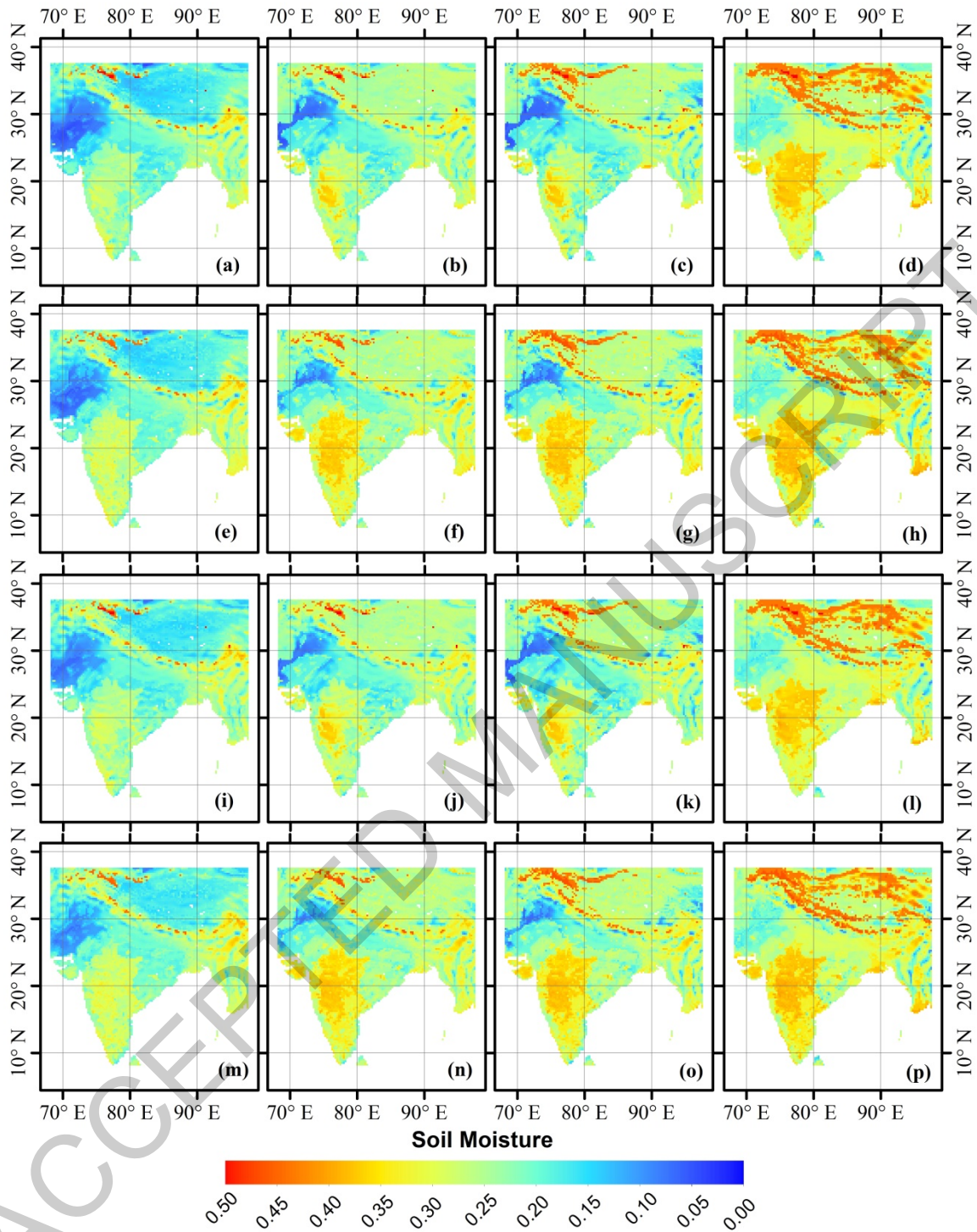


Figure 6. Variation in layer 1 soil moisture from OL and DA simulations compared to ISMN for August 2009: (a) from spin-up loop 1 and (b) from spin-up loop 4.

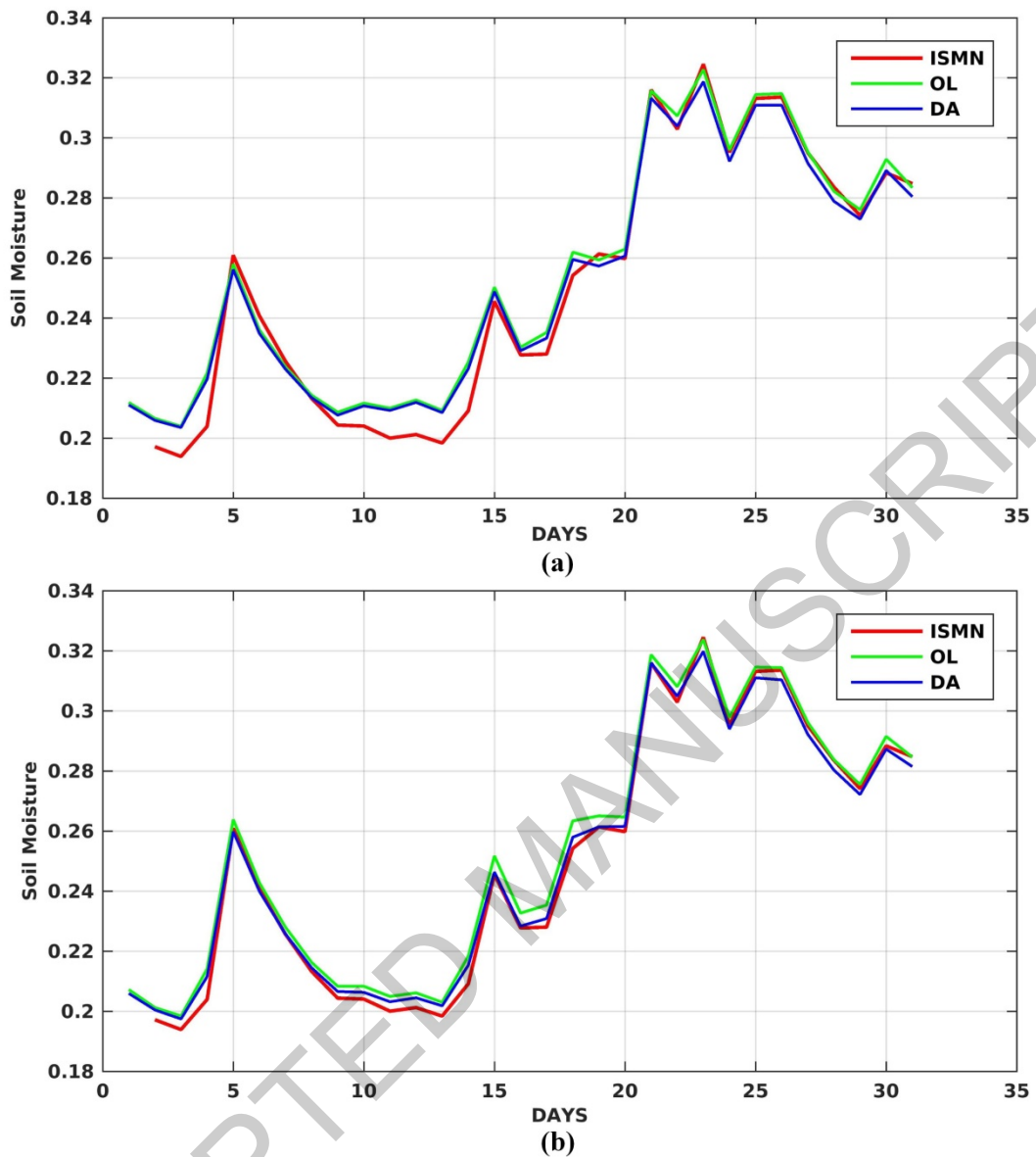


Figure 7. Variation in layer 1 soil moisture from OL and DA simulations compared to ISMN for September 2009: (a) from spin-up loop 1 and (b) from spin-up loop 4.

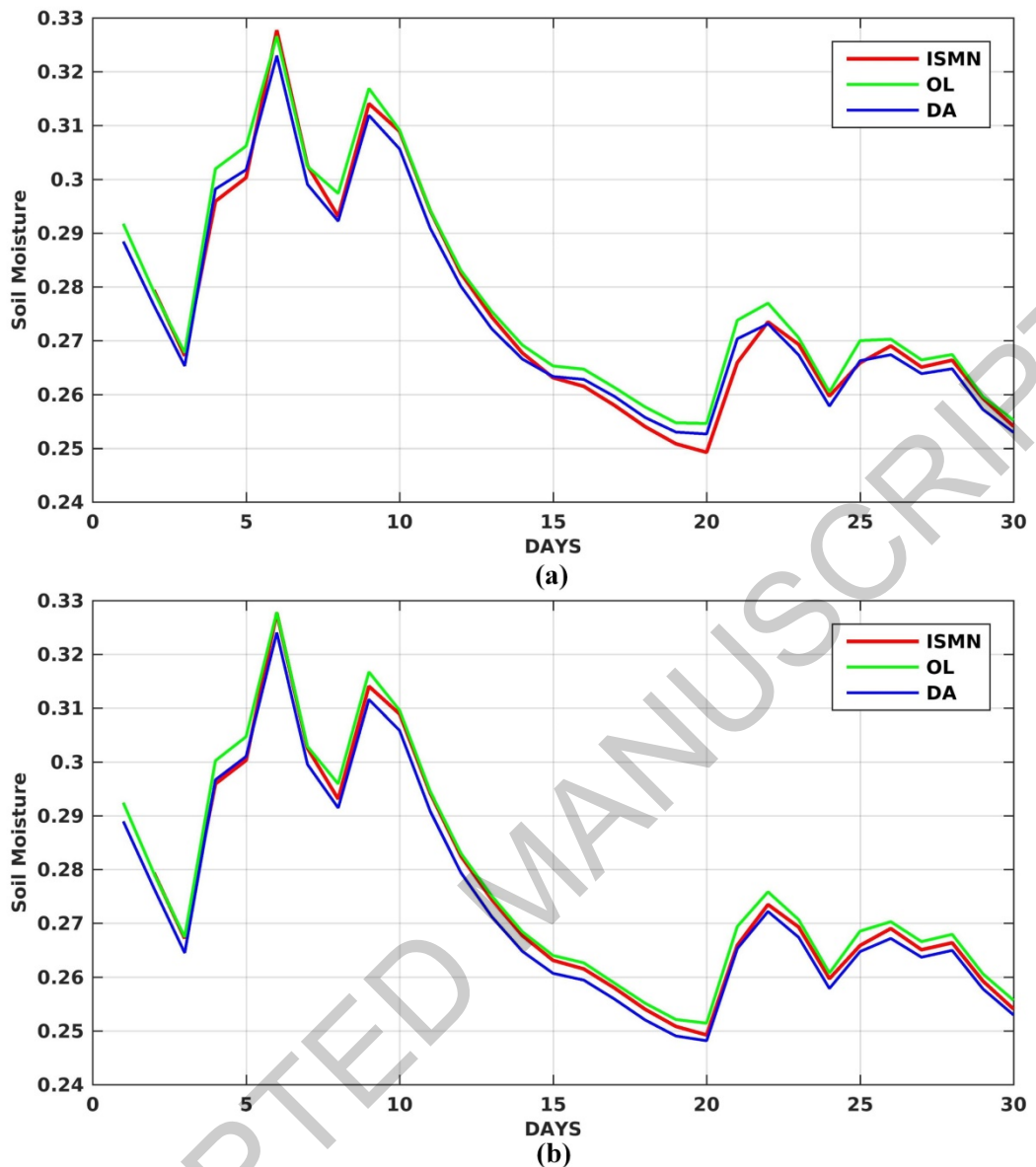


Figure 8. Experimental domain with coastlines and topographic heights of the model orography.

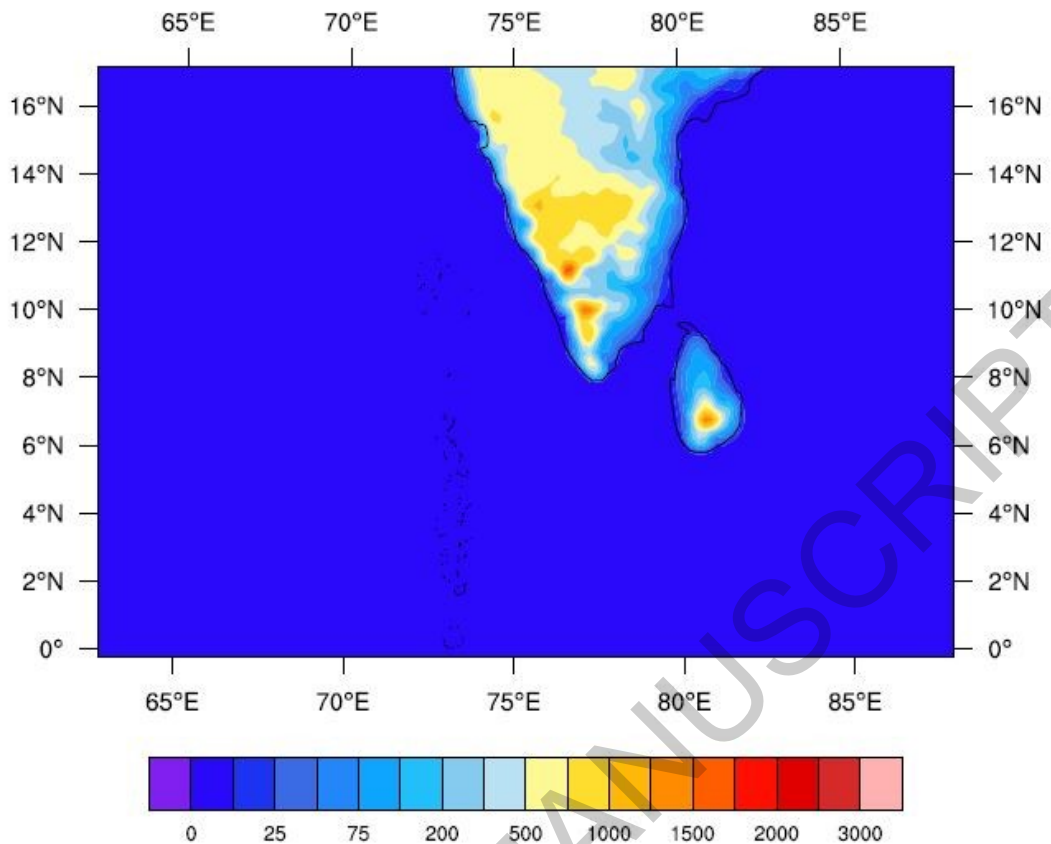


Figure 9. Time bars of WRF cycle runs, where 3DVAR assimilation includes assimilation of GTS data.

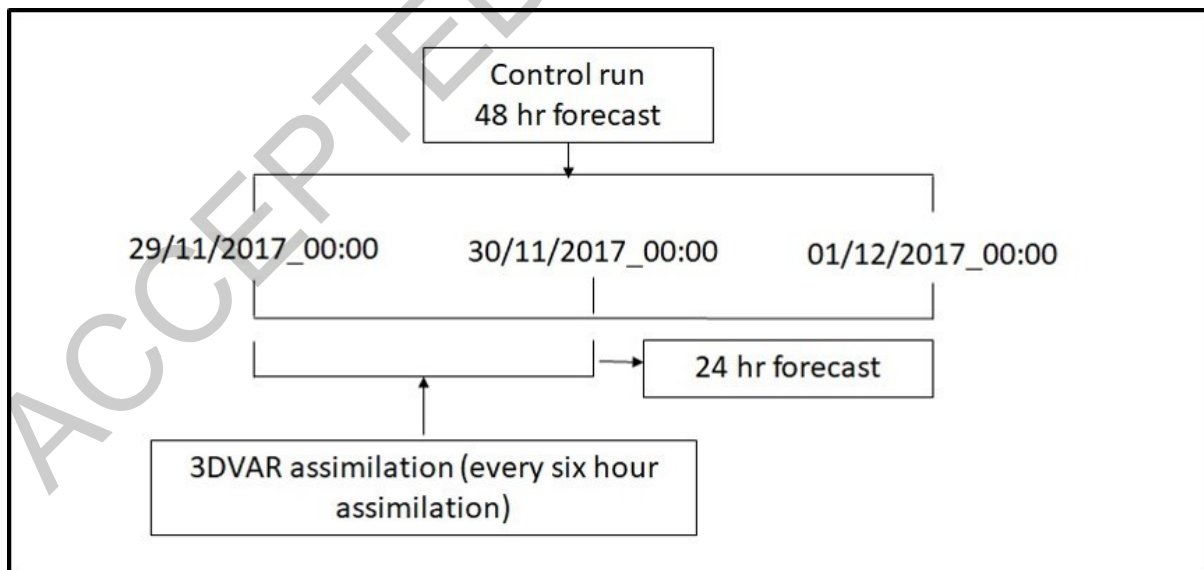


Figure 10. Six-hour accumulated precipitation of Kessler-BMJ experiment from: (a)–(d) control, (e)–(h) GTS, and (i)–(l) GPM observations. See Appendix for results of the remaining experiments.

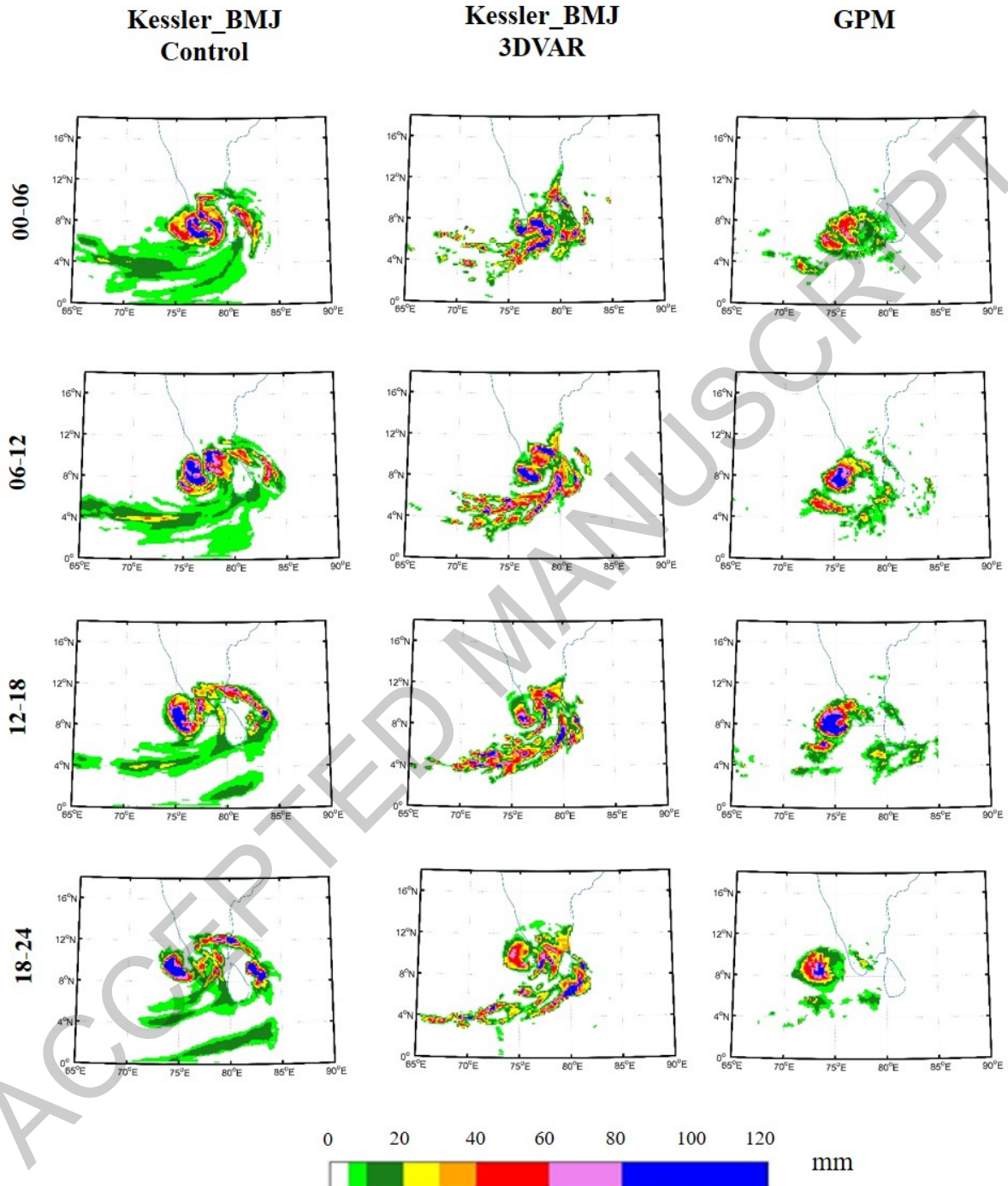
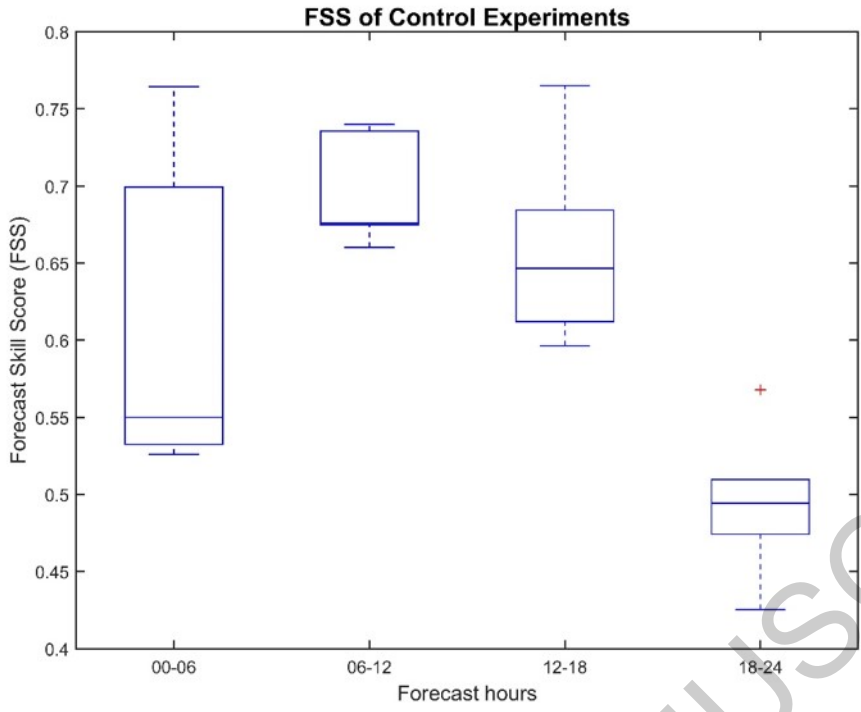
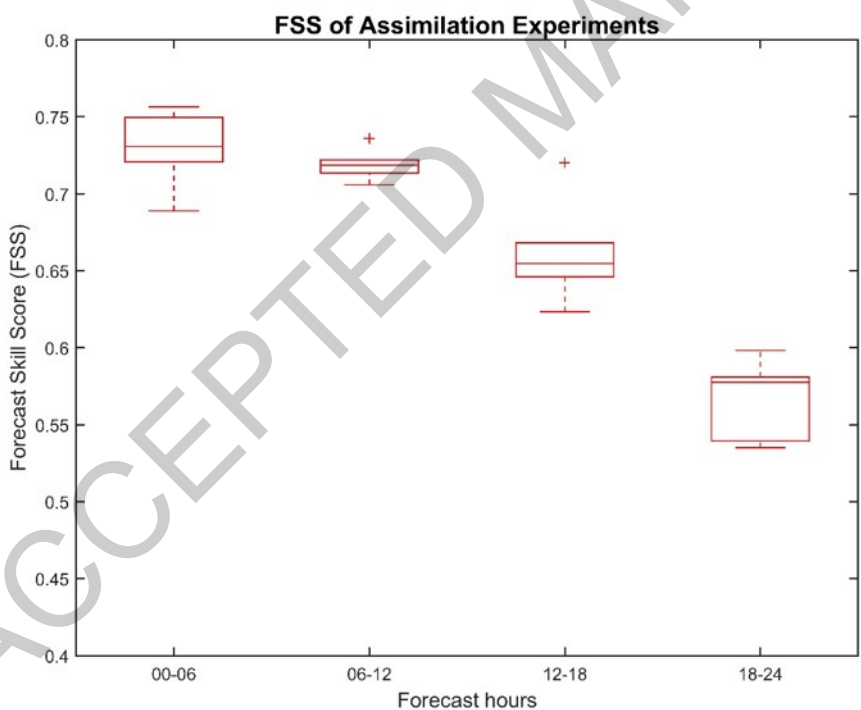


Figure 11. (a) FSS boxplots of control experiments and (b) FSS boxplots of assimilation experiments.



(a)



(b)

Figure 12. The track of Vardah Cyclone over the Bay of Bengal. The location of AMSR-2 observations near the eye of cyclone are shown by the red dot.

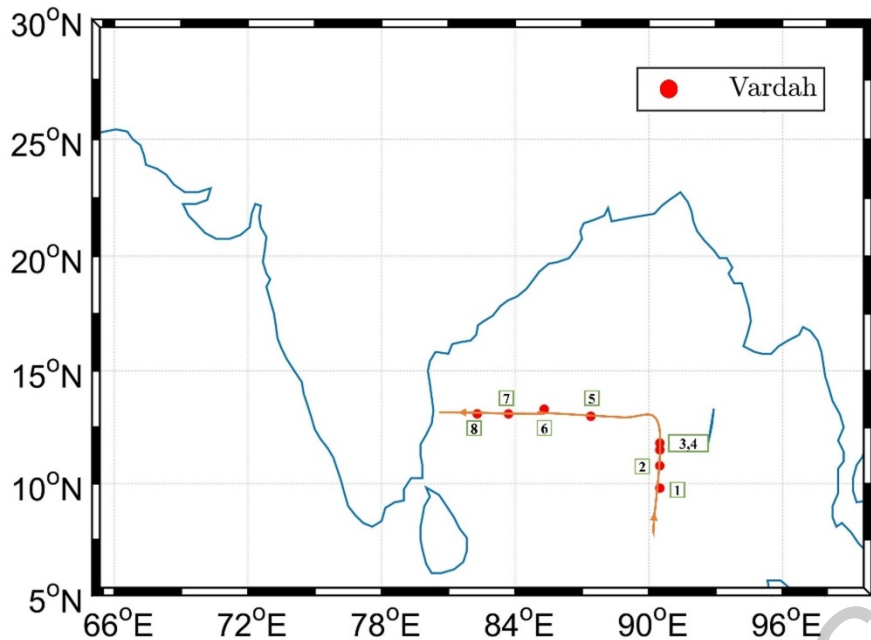


Figure 13. Flow diagram of AMSR-2 all-sky radiance simulation using WRF forecasts and RTToV-SCATT model. The mie-tables consists the database of optical properties for each DDA shape.

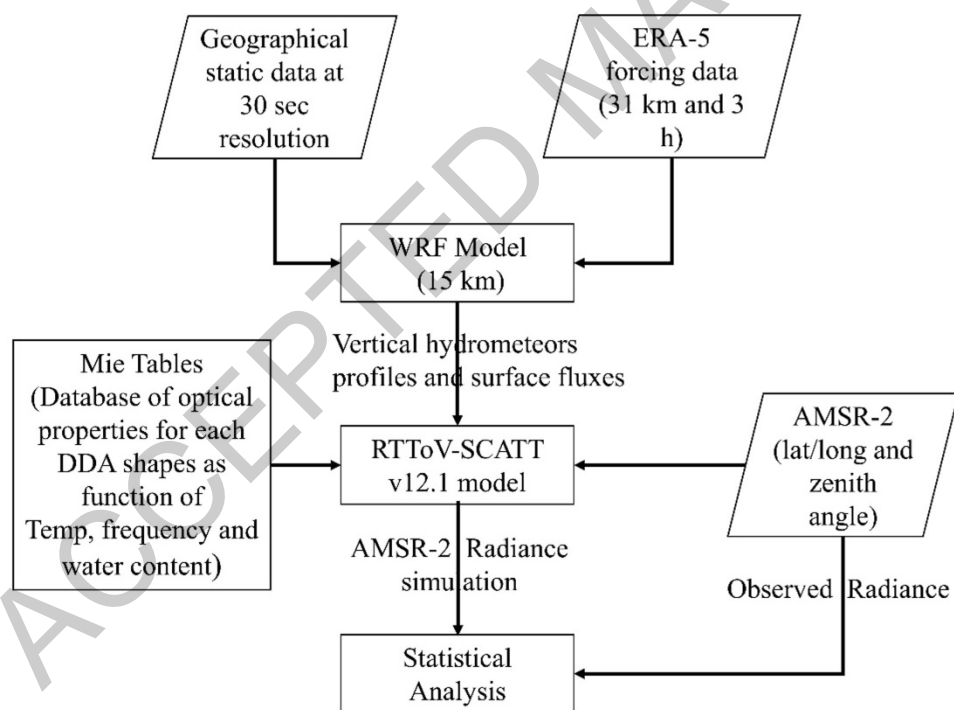


Figure 14. (a) Brightness temperature (BT) of observations at 89V of AMSR-2 and simulated BTs, with (b) mie-spheres and DDA shapes, (c) sector snowflake, (d) six-bullet rosette, (e) block-column and (f) thin-plate for the Vardah Cyclone (6–12 December 2016).

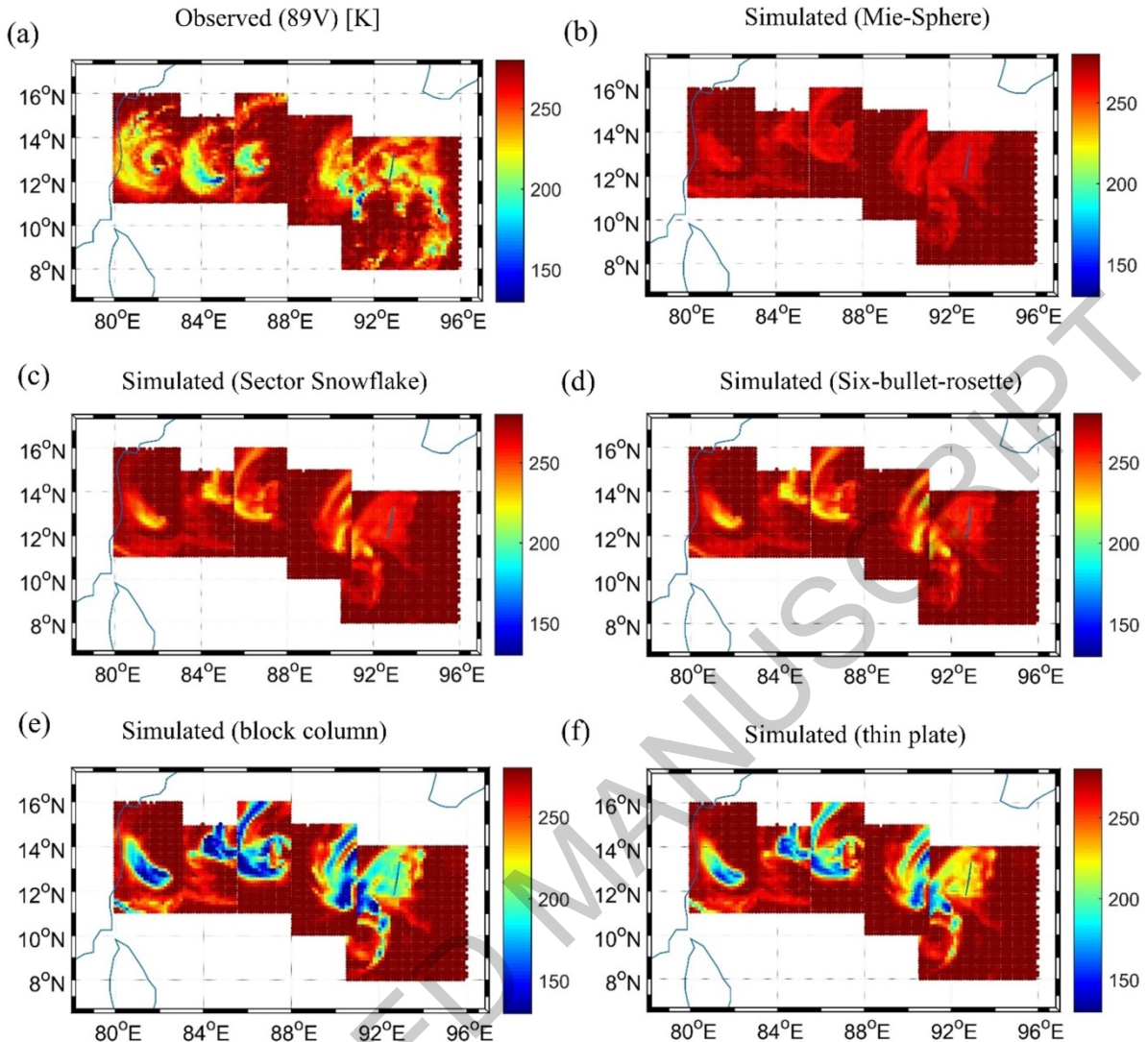


Figure 15. Measure of the goodness of fit between observed and simulated BTs: (a) log of the ratio of histograms (simulation divided by the observation) for mie-sphere and four DDA shapes; the bin size is 2.5K. (b) Skewness of O-B values. Thin-plate have the finest results for Vardah cyclone over Bay of Bengal.

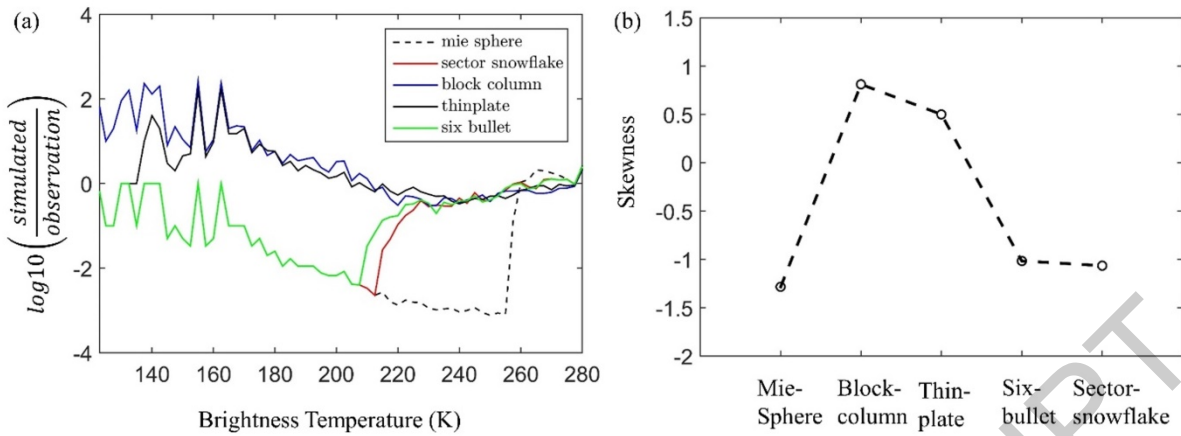


Table 1. Description of the experiments.

No.	Experiment	Description		
		Microphysics scheme	Cumulus scheme	Assimilation
1	Kessler-BMJ control	Kessler	Betts-Miller-Janjic	No
2	Kessler- G3 control	Kessler	Grell 3D	No
3	Kessler-KFm control	Kessler	Modified Kain-Fritsch	No
4	LIN-BMJ control	Lin et al	Betts-Miller-Janjic	No
5	LIN- G3 control	Lin et al	Grell 3D	No
6	LIN-KFm control	Lin et al	Modified Kain-Fritsch	No
7	Kessler-BMJ 3DVAR	Kessler	Betts-Miller-Janjic	GTS data
8	Kessler- G3 3DVAR	Kessler	Grell 3D	GTS data
9	Kessler-KFm 3DVAR	Kessler	Modified Kain-Fritsch	GTS data
10	LIN-BMJ 3DVAR	Lin et al	Betts-Miller-Janjic	GTS data
11	LIN- G3 3DVAR	Lin et al	Grell 3D	GTS data
12	LIN-KFm 3DVAR	Lin et al	Modified Kain-Fritsch	GTS data

Table 2. Forecast skill score of the experiments.

Experiment	Forecast skill score			
	00–06	06–12	12–18	18–24
Kessler-BMJ control	0.549186	0.676123	0.612154	0.425423
Kessler- G3 control	0.532495	0.674809	0.647583	0.47421
Kessler-KFm control	0.699322	0.739942	0.684311	0.509712
LIN-BMJ control	0.550901	0.675686	0.596431	0.506864
LIN- G3 control	0.525911	0.660205	0.645718	0.481745
LIN-KFm control	0.764478	0.735632	0.765116	0.567723
Kessler-BMJ 3DVAR	0.756488	0.72203	0.668142	0.577071
Kessler- G3 3DVAR	0.727988	0.735791	0.653906	0.578157
Kessler-KFm 3DVAR	0.688855	0.7135	0.72004	0.598202
LIN-BMJ 3DVAR	0.749522	0.715739	0.6555	0.580952
LIN- G3 3DVAR	0.720665	0.721514	0.623349	0.539393
LIN-KFm 3DVAR	0.733276	0.705772	0.646146	0.535125

Table 3. WRF model configuration over Bay of Bengal (Routray *et al.*, 2016)

Map projection	Mercator
Horizontal grid system	Arakawa C-grid
Microphysics	WRF single moment 6-class microphysics scheme (Hong and Lim 2006)
Convection	Kain-Fritsch scheme (Kain 2004)
Planetary boundary layer	Yonsei scheme (Hong <i>et al.</i> 2006)
Shortwave radiation scheme	Dudhia scheme (Dudhia 1989)
Long-wave radiation	Rapid Radiative Transfer Model Scheme (Mlawer <i>et al.</i> 1997)
Land surface model	Noah scheme (Tewari <i>et al.</i> 2004)

Table 4 The lowest depression of simulated BTs, h parameter and skewness corresponding to snow particles DDA shapes for Vardah Cyclone.

DDA shape for snow hydrometeors	Lowest temperature of simulated BT	H value	Skewness of O-B error
Mie-sphere	255K	1.6997	-1.2840
Sector snowflake	213K	1.0092	-1.0646
Six-bullet rosette	208K	0.9389	-1.0165
Block column	100K	0.7876	0.8114
Thin plate	134K	0.4941	0.5008

Appendix

Results of the case study on atmospheric data assimilation

The first experiment results are shown in Figure 15. The remaining experiments are presented below.

Figure A1. Six-hour accumulated precipitation of Kessler-G3 experiment from: (a)–(d) control, (e)–(h) GTS, and (i)–(l) GPM observations.

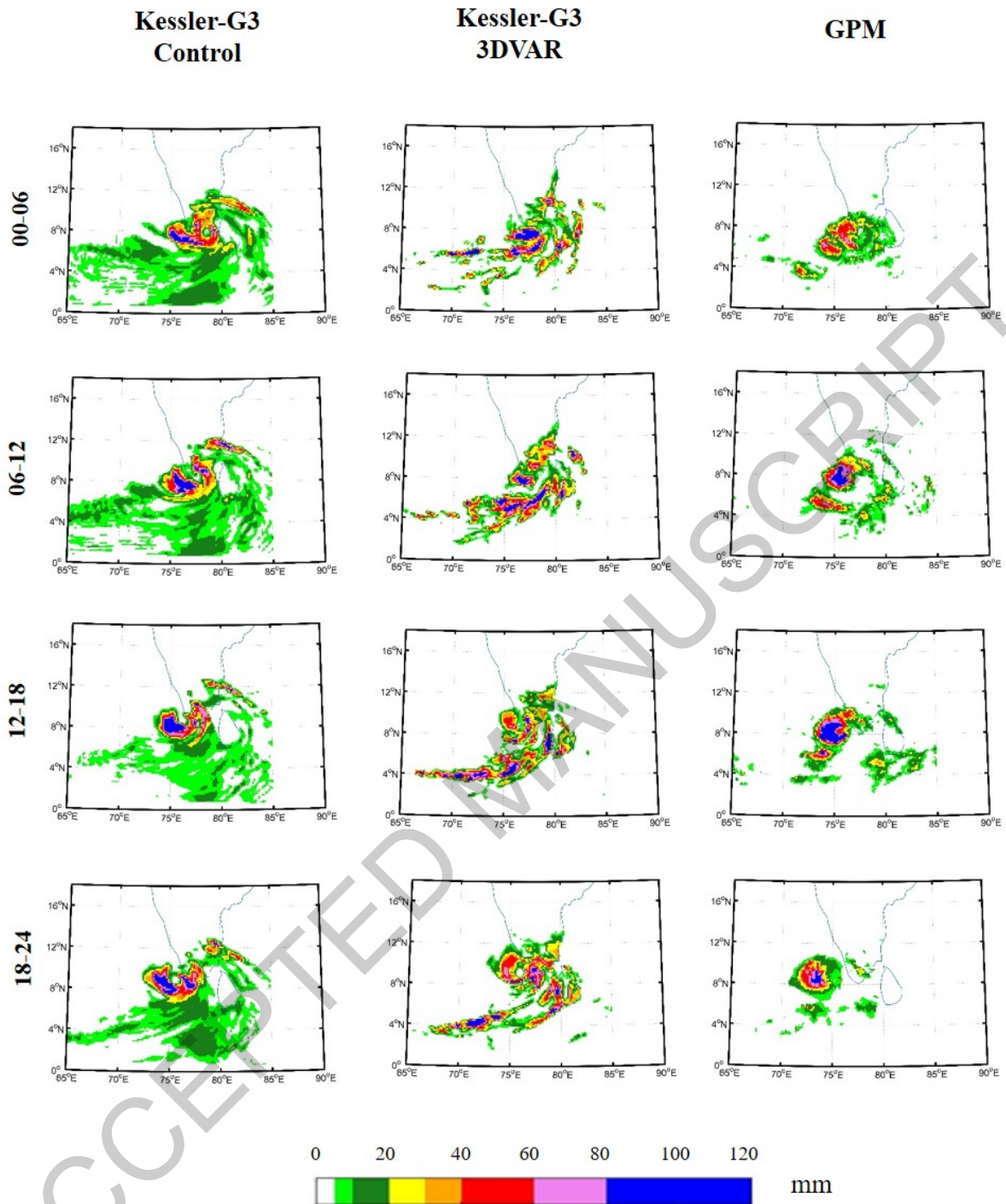


Figure A2. Six-hour accumulated precipitation of Kessler-KFm experiment from: (a)–(d) control, (e)–(h) GTS, and (i)–(l) GPM observations.

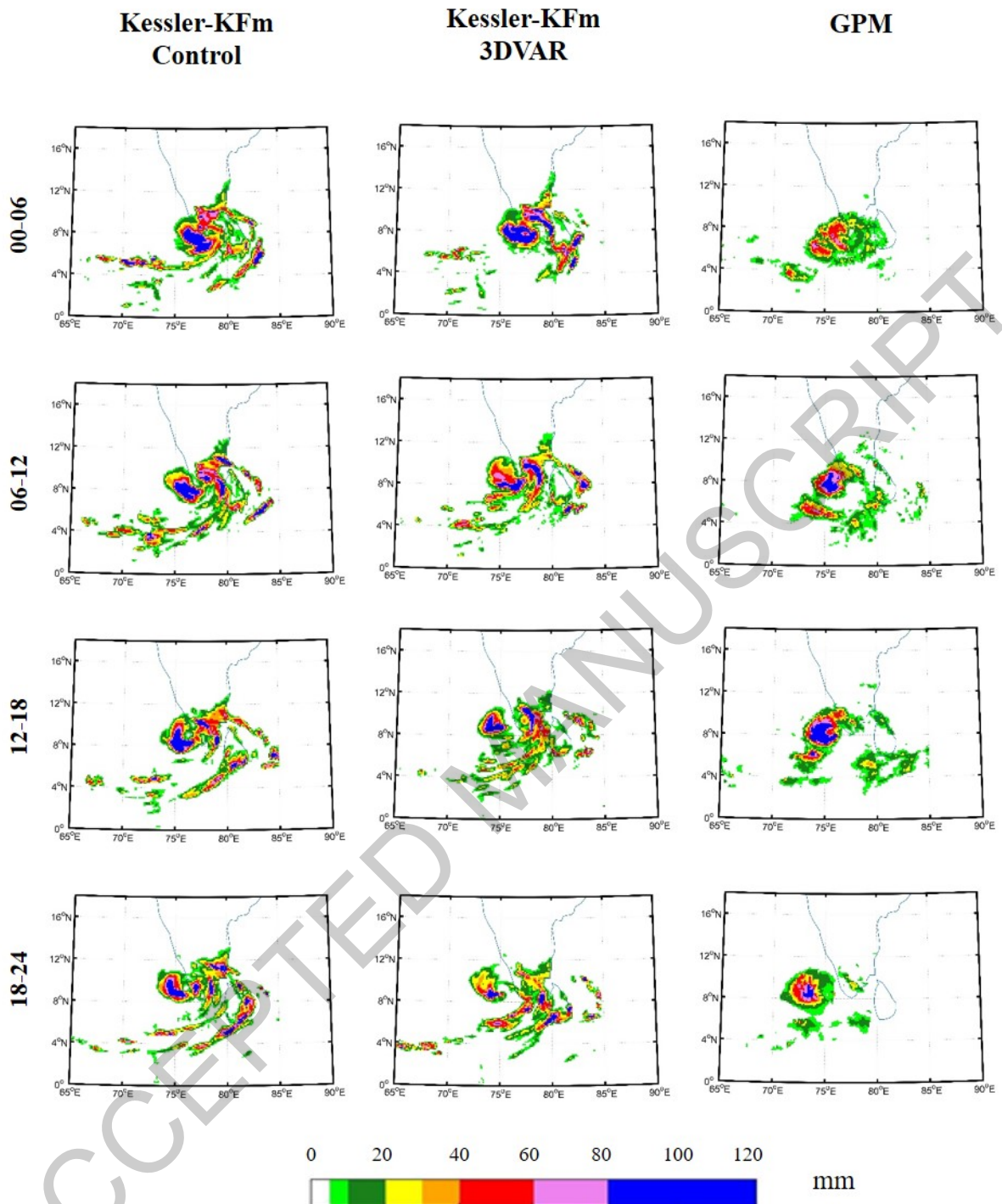


Figure A3. Six-hour accumulated precipitation of LIN-BMJ experiment from: (a)–(d) control, (e)–(h) GTS, and (i)–(l) GPM observations.

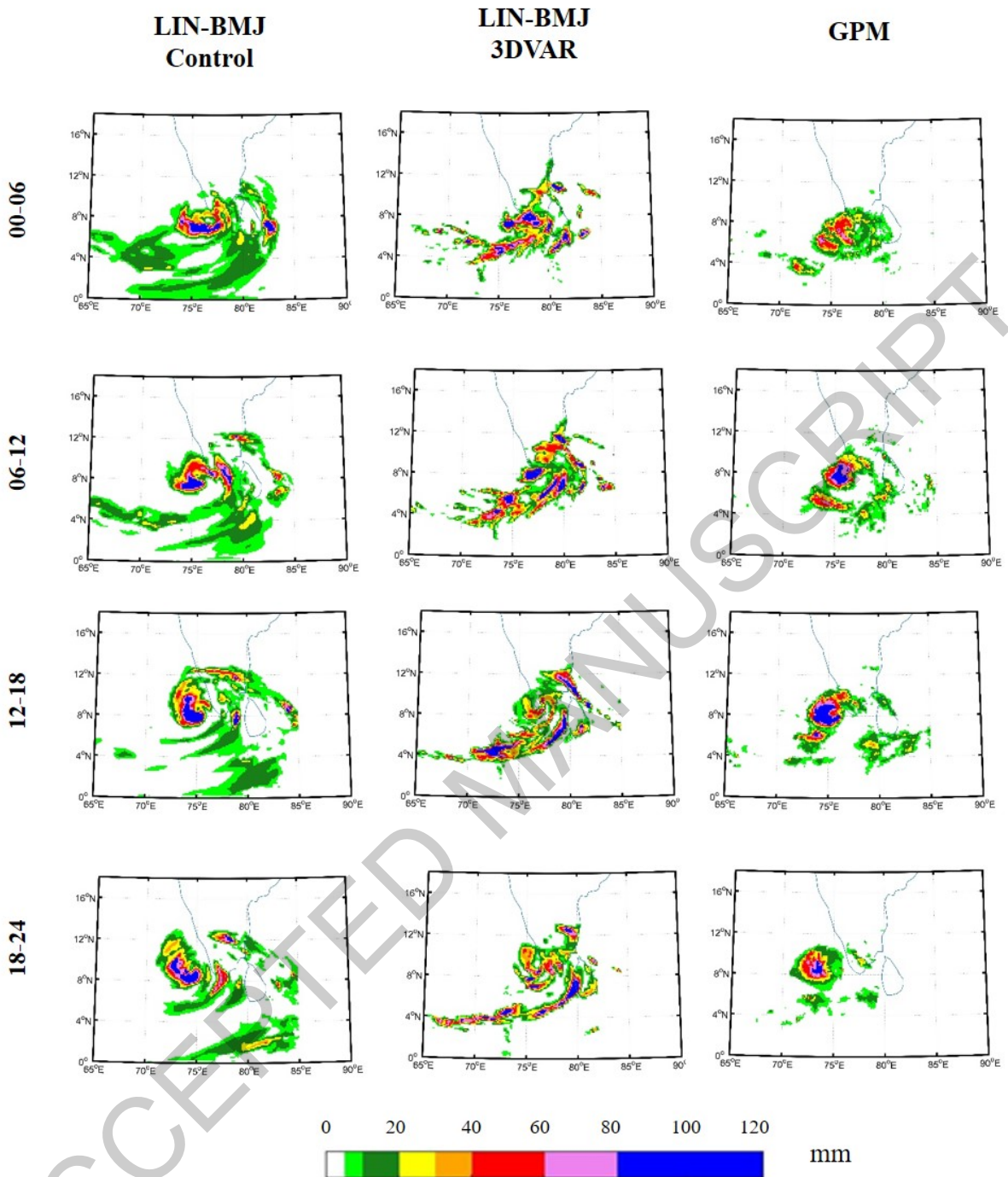


Figure A4. Six-hour accumulated precipitation of LIN-G3 experiment from: (a)–(d) control, (e)–(h) GTS, and (i)–(l) GPM observations.

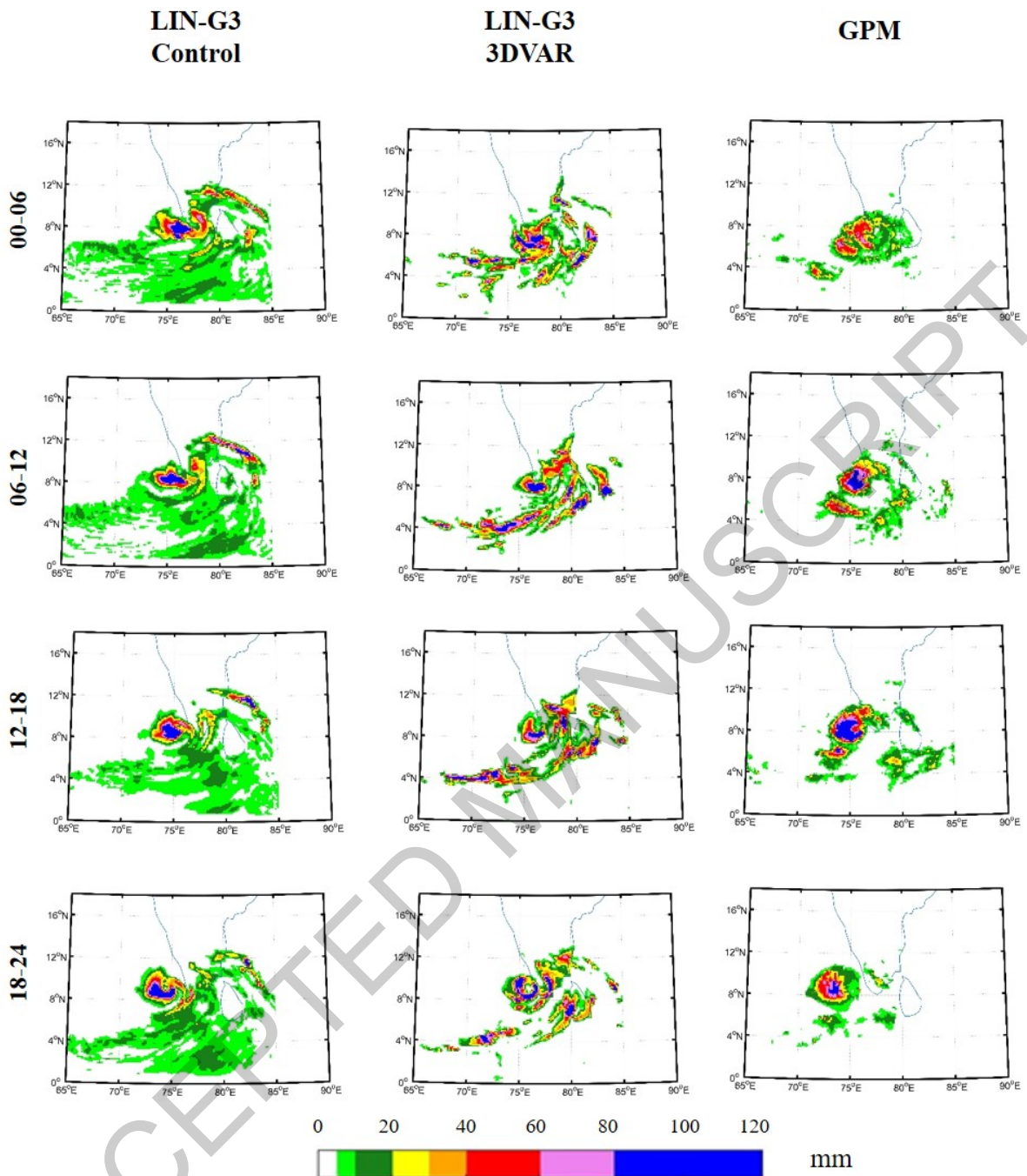


Figure A5. Six-hour accumulated precipitation of LIN-KFm experiment from: (a)–(d) control, (e)–(h) GTS, and (i)–(l) GPM observations.

